Energy, Water Flux & Carbon Cycle

Weiqiang Ma

ITP, CAS

2019.11.21

Chongqing

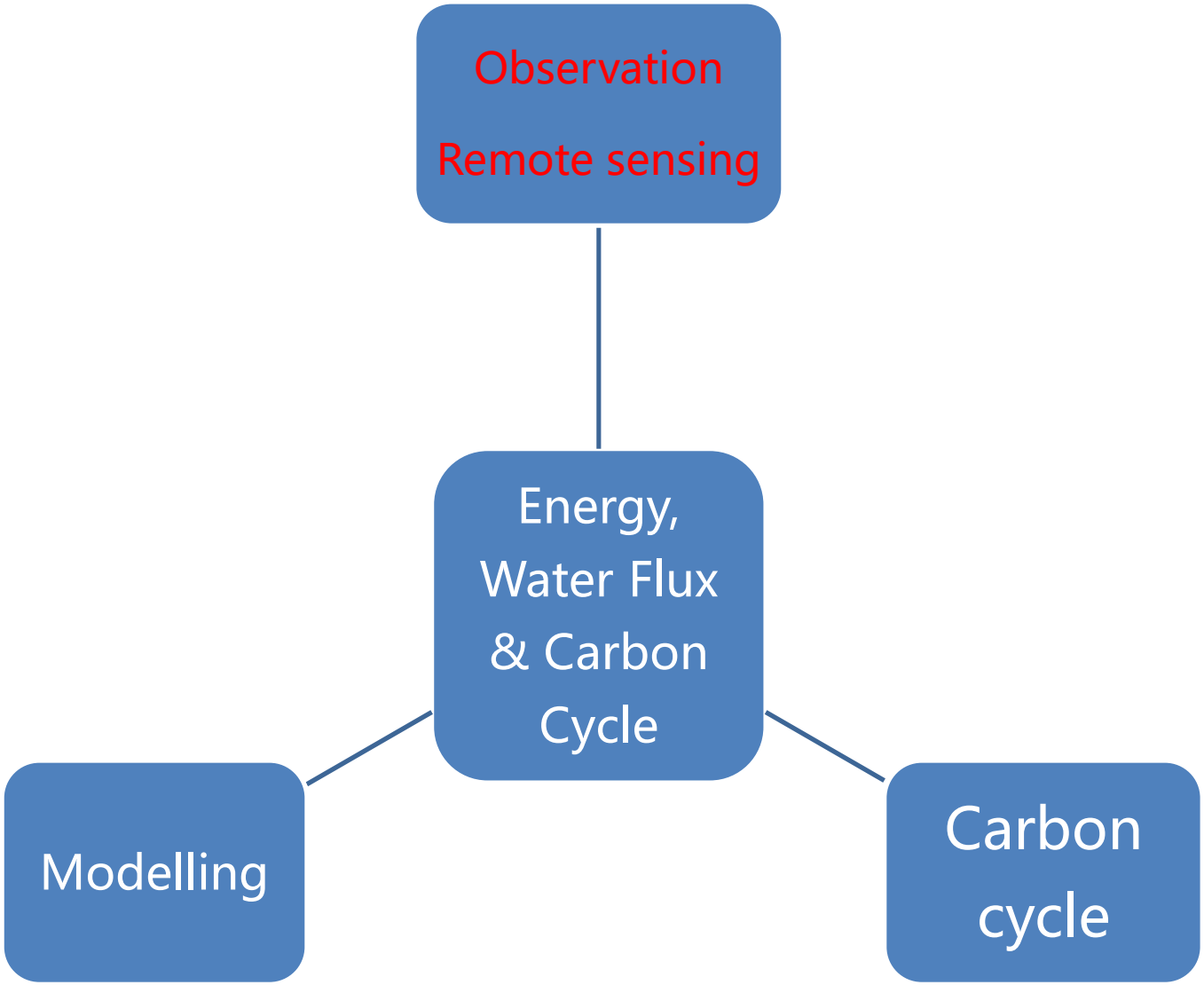
Observation
Remote sensing
Energy, Water Flux & Carbon Cycle
Modelling
Carbon cycle

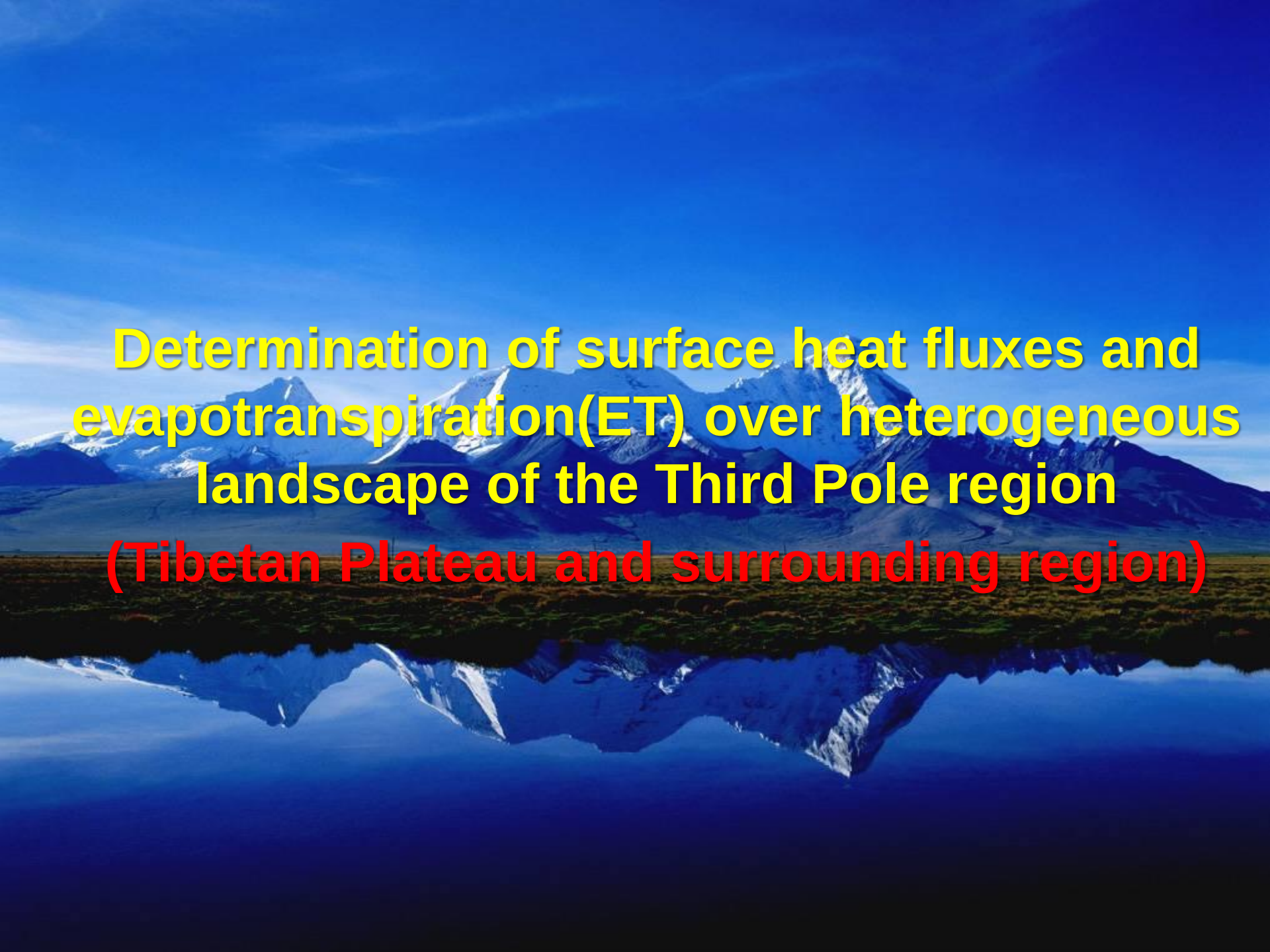
Determination of surface heat fluxes and evapotranspiration(ET) over heterogeneous landscape of the Third Pole region
(Tibetan Plateau and surrounding region)

Why do we have this kind of study?

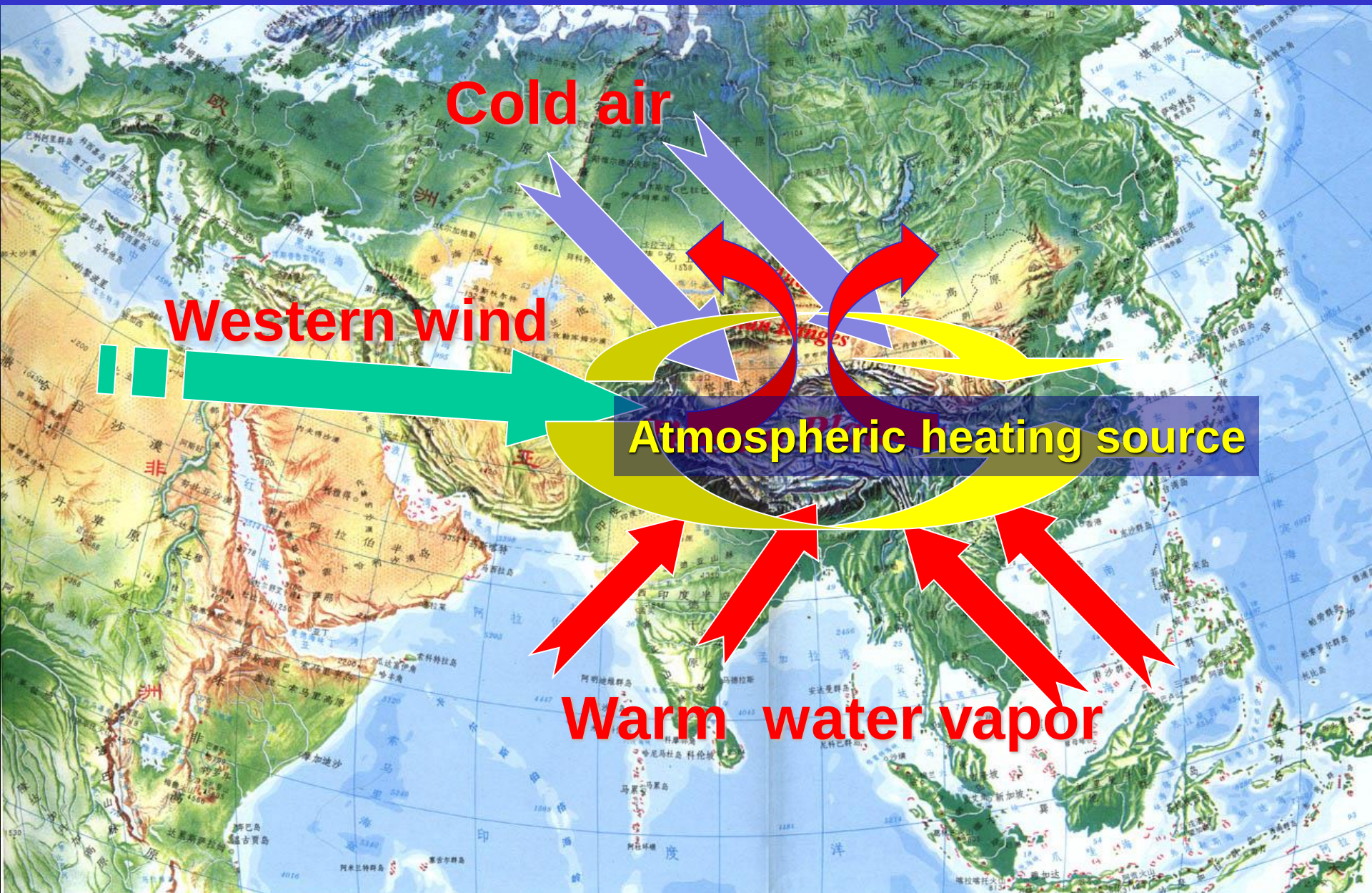

Tibetan Plateau

Heating to the atmosphere

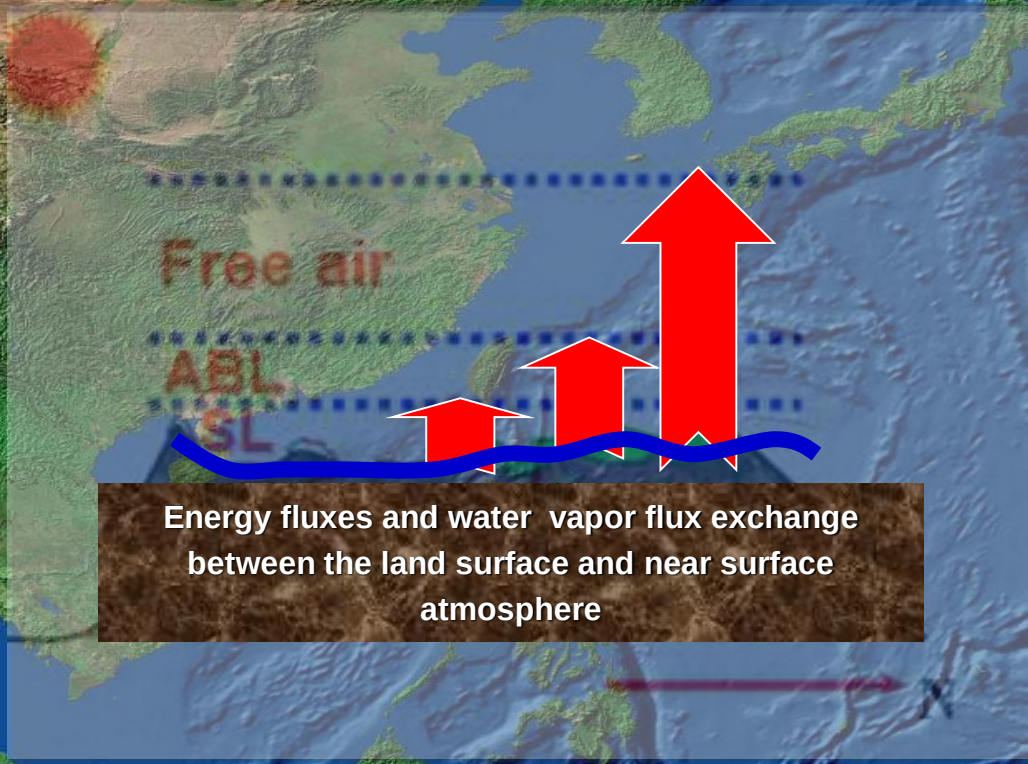

Energy fluxes and water vapor flux exchange between the land surface and near surface atmosphere


Heterogeneous land surface(different ecosystems)
Plateau Mountain
How to get the regional surface heat fluxes and ET over the Third Pole region
??????????
Desertification grass-land
Glacier (snow mountain)
Plateau lake
Farm-land
Wet-land


1.
Set up observation stations at different land surfaces(ecosystems)
Observation
Data analysis
Heat fluxes and ET at eac land surface
2.
Satellite data
Parameterization
understanding of regional surface fluxes and ET over the Third Pole region
3.
Models
Modeling
4.
LDAS

Tibetan Observation and Research Platform

---TORP


Mt. Mushitageta
Haibei
Ali
Golmud
Shuanghu
Mt. Tanggula
Meso Scale Experimental Area
Nam Co
Lhasa
Mt. Gongga
Mt. Qomolangma(Everest)
Motuo
Linzhi
Constructed stations, ITP,CAS
Planning stations, ITP,CAS
Constructed stations, another institutes, CAS

7 ITP/CAS comprehensive observation stations in TP

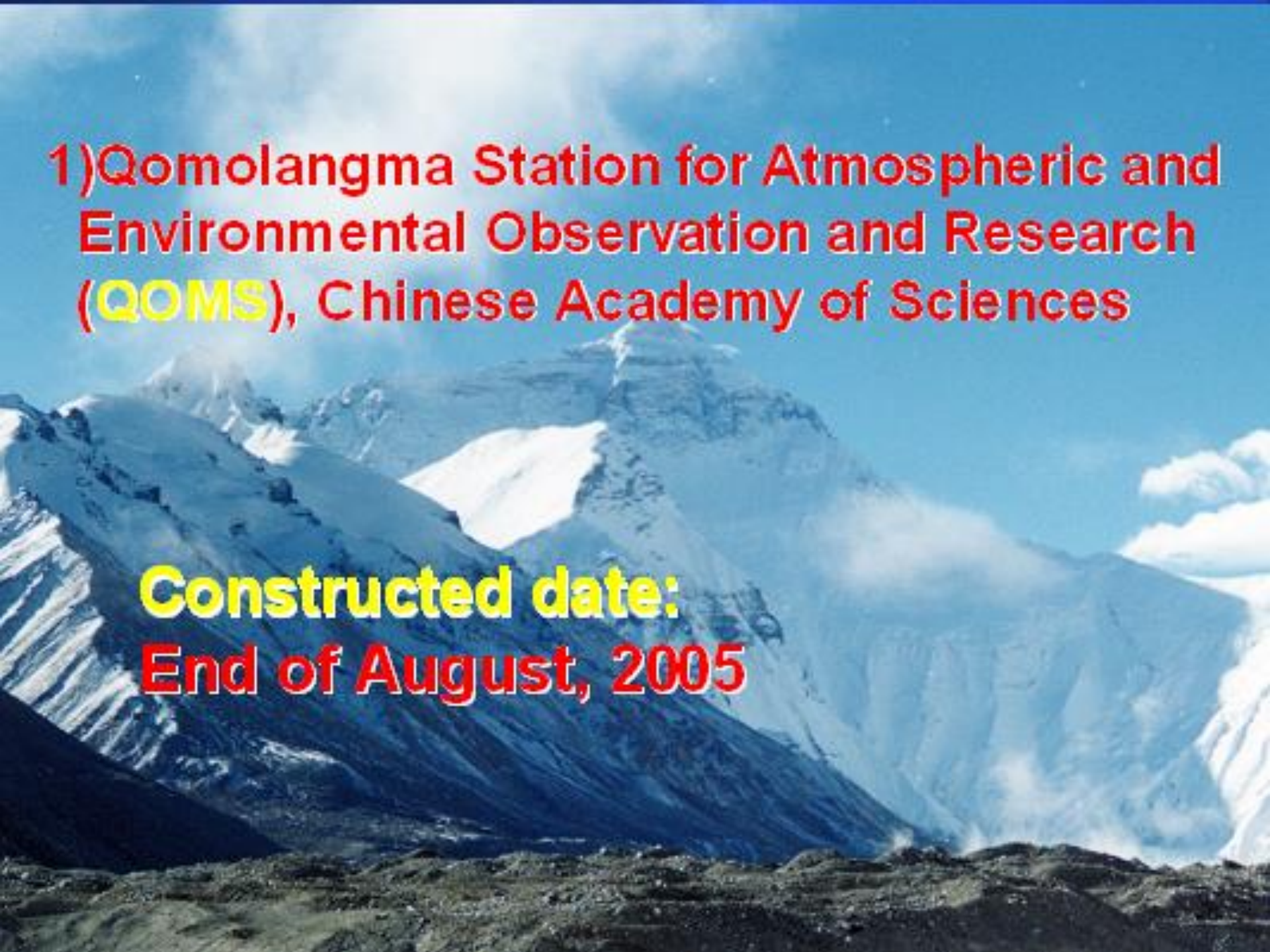
1)Qomolangma Station for Atmospheric and Environmental Observation and Research (QOMS), Chinese Academy of Sciences
Constructed date:
End of August, 2005

Qomolangma St.

高山大气与环境过程

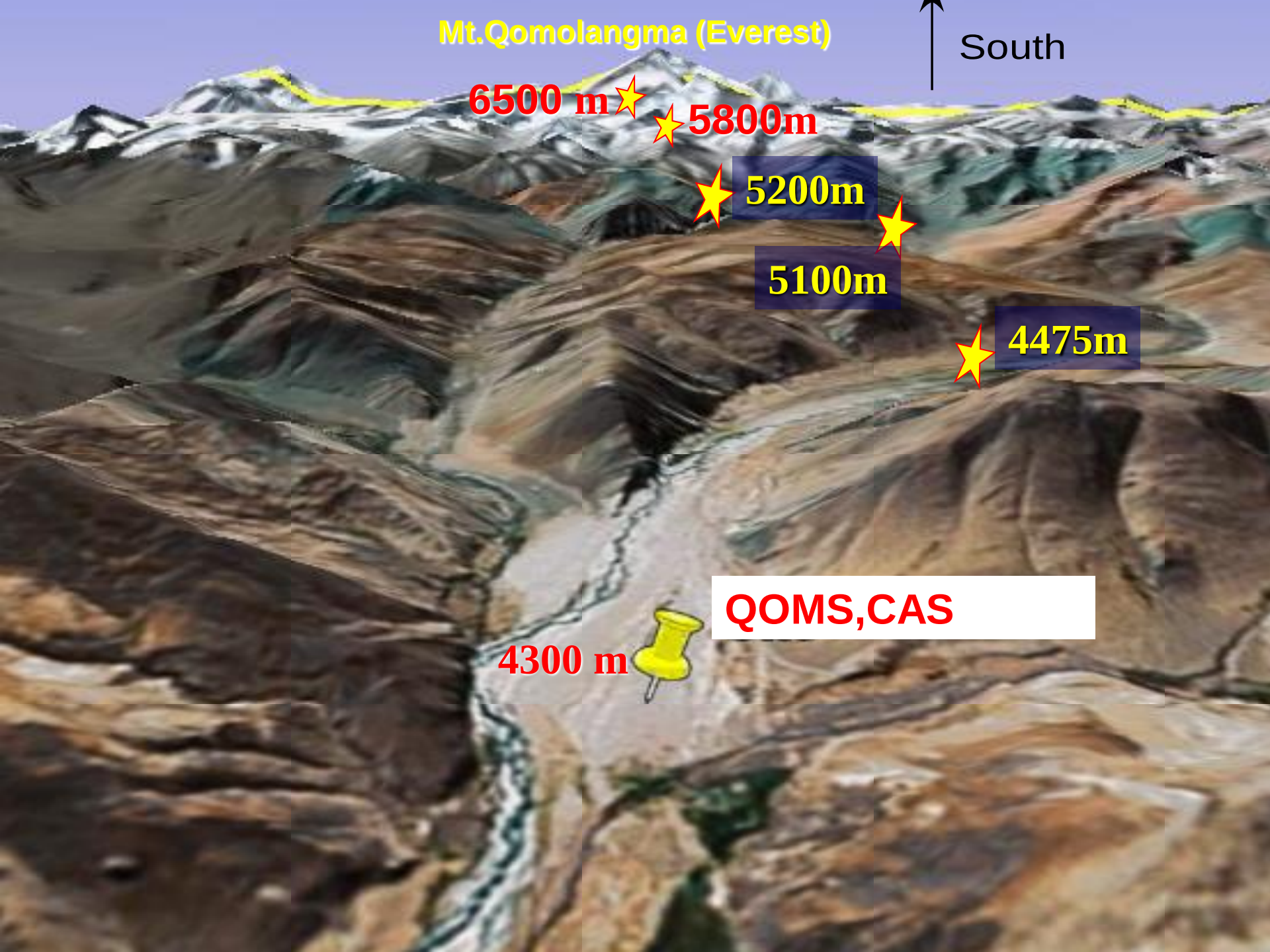
Mt.Qomolangma (Everest)
South
6500 m
5800m
5200m
5100m
4475m
QOMS,CAS
4300 m


40m PBL tower
(radiation system and SMTMS)

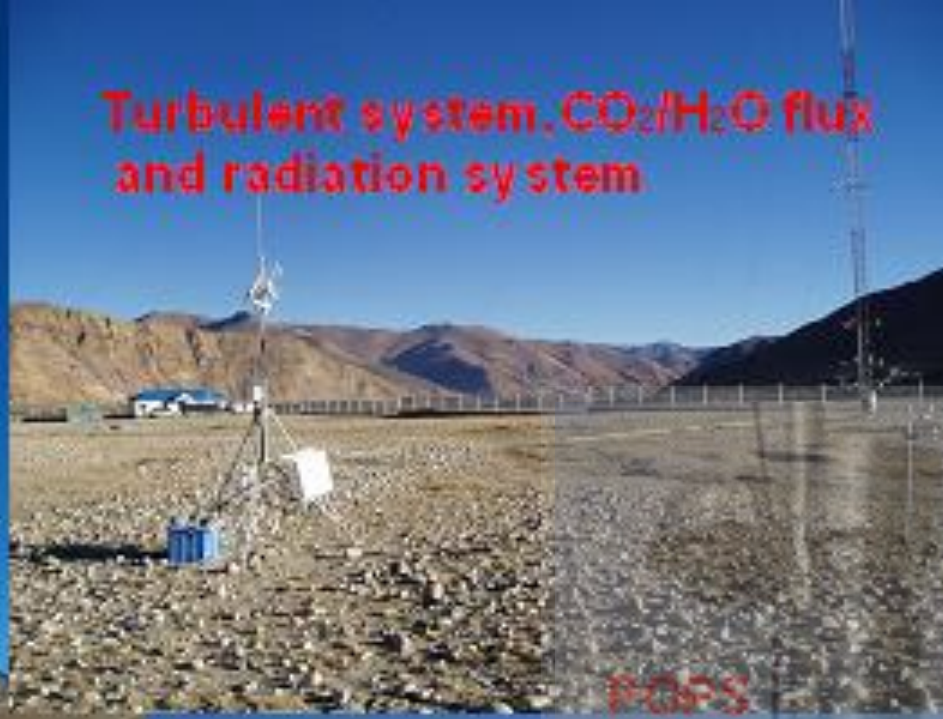
Turbulent system.CO2/H2O flux
and radiation system
P-GPS


Wind Profiler and RASS


GPS


Turbulent system,CO2/H2O flux
and radiation system
6500m

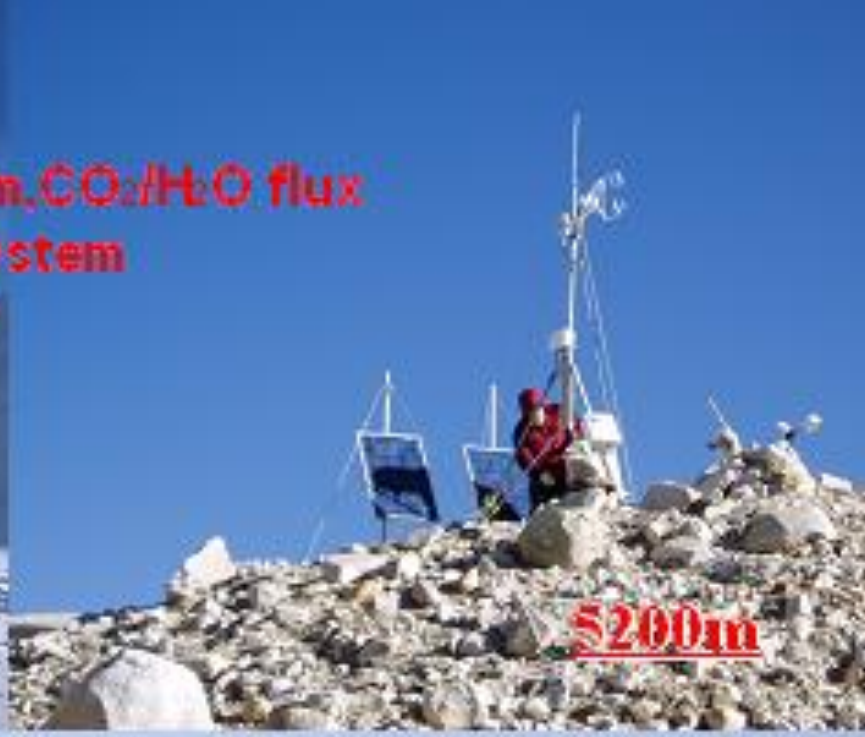
5200m


4475m


Radio sonde system
5200m


2). Nam Co Station for Multisphere Observation and Research (NAMOR), Chinese Academy of Sciences
Nam Co Station
Constructed date:
End of September, 2005

Nam Co St.

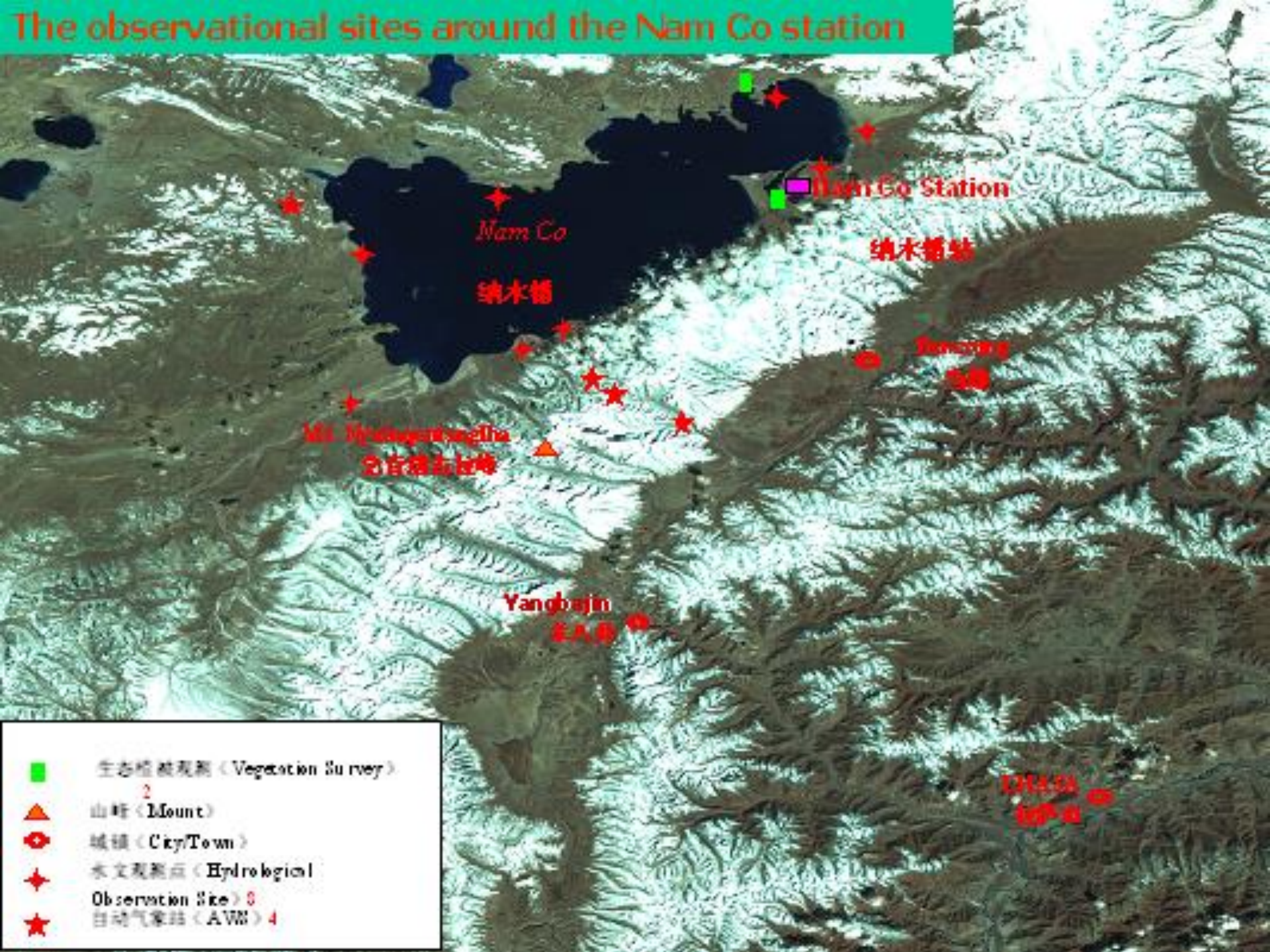
The observational sites around the Nam Co station
Nam Co Station
Nam Co
Yangbajin
生态植被观测（Vegetation Survey）
2
山峰（Mount）
城镇（City/Town）
水文观测点（Hydrological
Observation Site）8
自动气象站（AWS）4

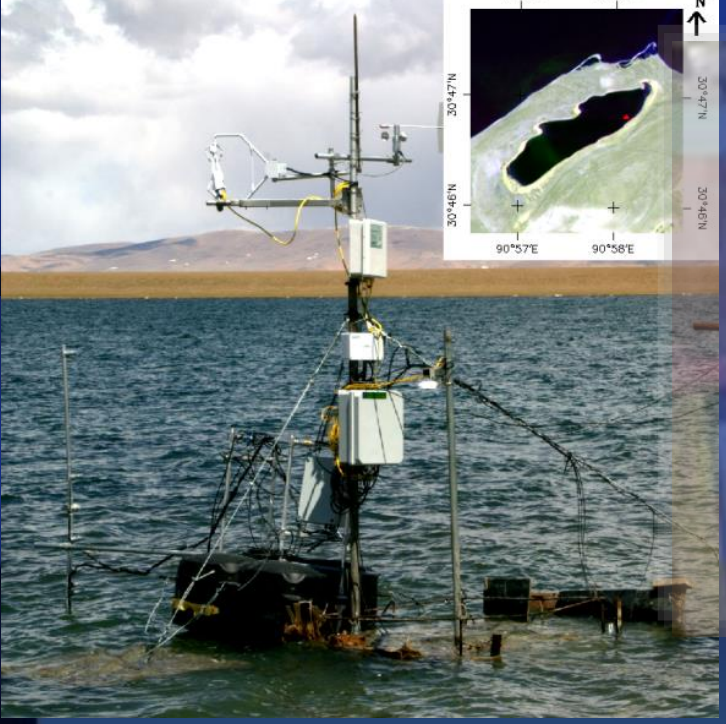

POPS

Aerosol Sampler

2005 6 7

52m PBL tower
(Radiation system
and SMTMS)

Turbulent system, CO_2/H_2O flux and radiation system


AWS around the
Nam co Station


Evaporation Observation

3). Southeast Tibet Station for Alpine Environment Observation and Research (SETS), CAS （Linzhi Station）

Constructed date: **Beginning of November, 2006**


20m PBL tower
(SMTMS)


Turbulent system &CO2/H2O flux


Kipp & Zonen
Radiation system

Ngari Station for Desert Environment Observation and Research, Chinese Academy of Sciences (NASDE/CAS)

Ngari Station for Desert Environment Observation and Research, Chinese Academy of Sciences (NASDE/CAS)

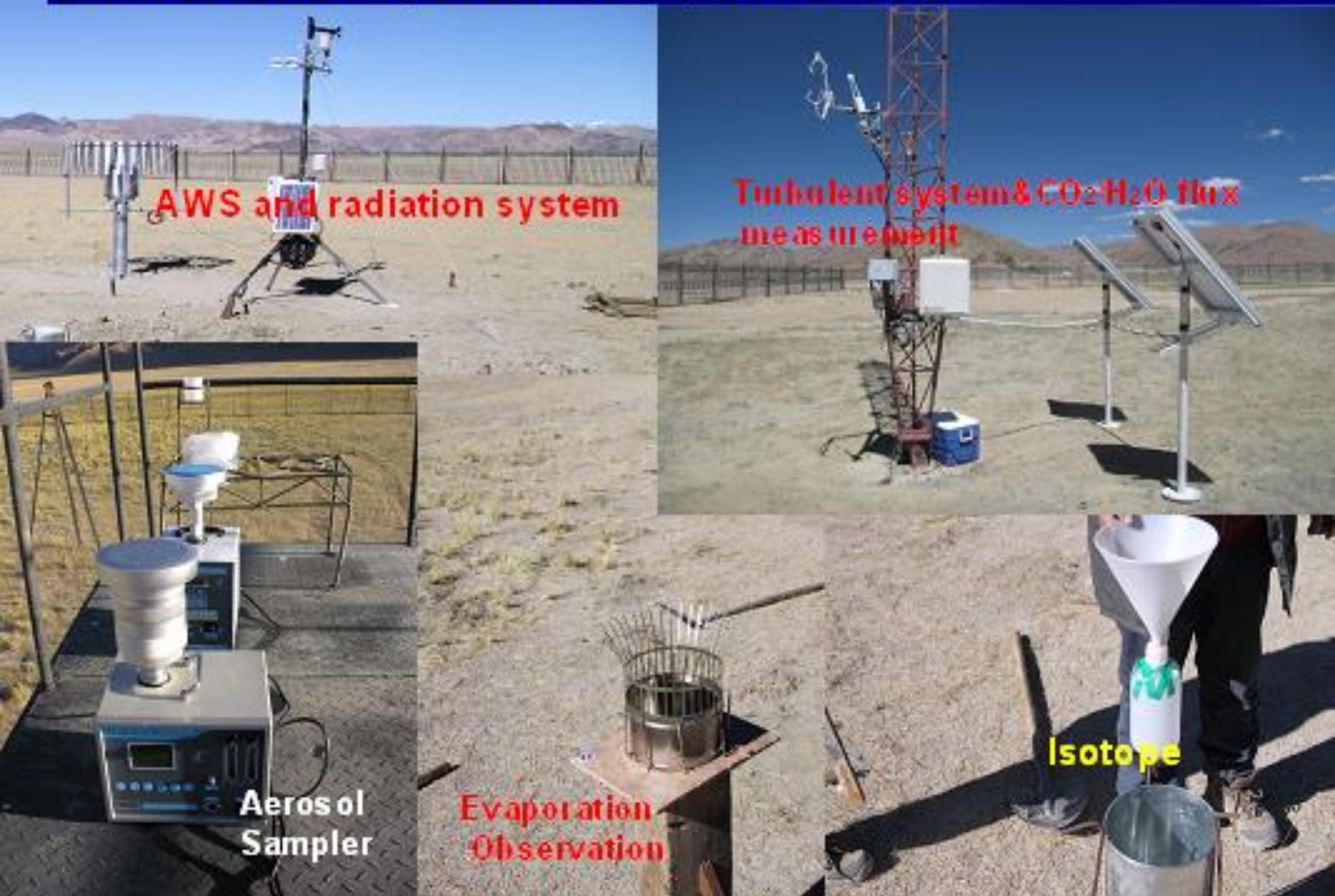

5）Muztagh Ata Station for Westerly Environment Observation and Research, Chinese Academy of Sciences (MASWE/CAS)

Muztagh Ata Station for Westerly Environment Observation and Research, Chinese Academy of Sciences (MASWE/CAS)

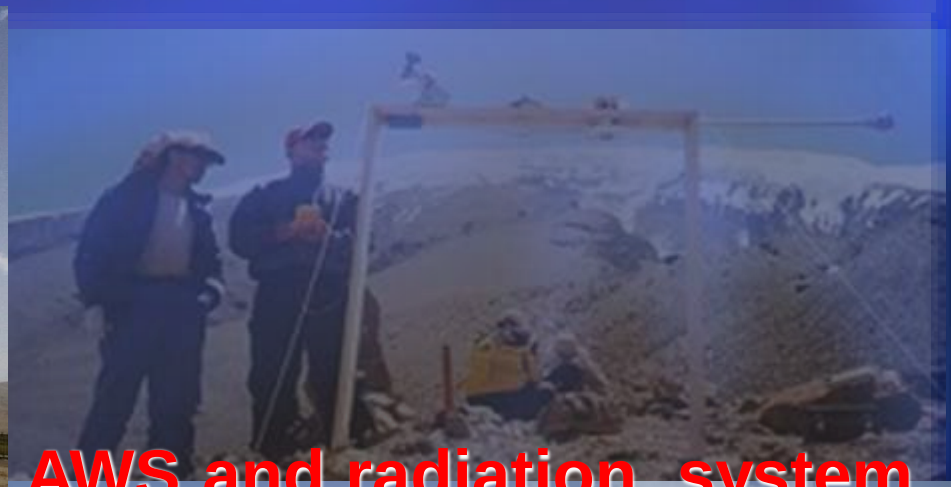

AWS and radiation system

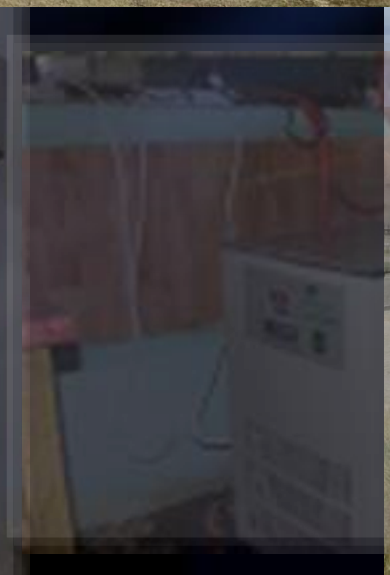

Shuanghu Station

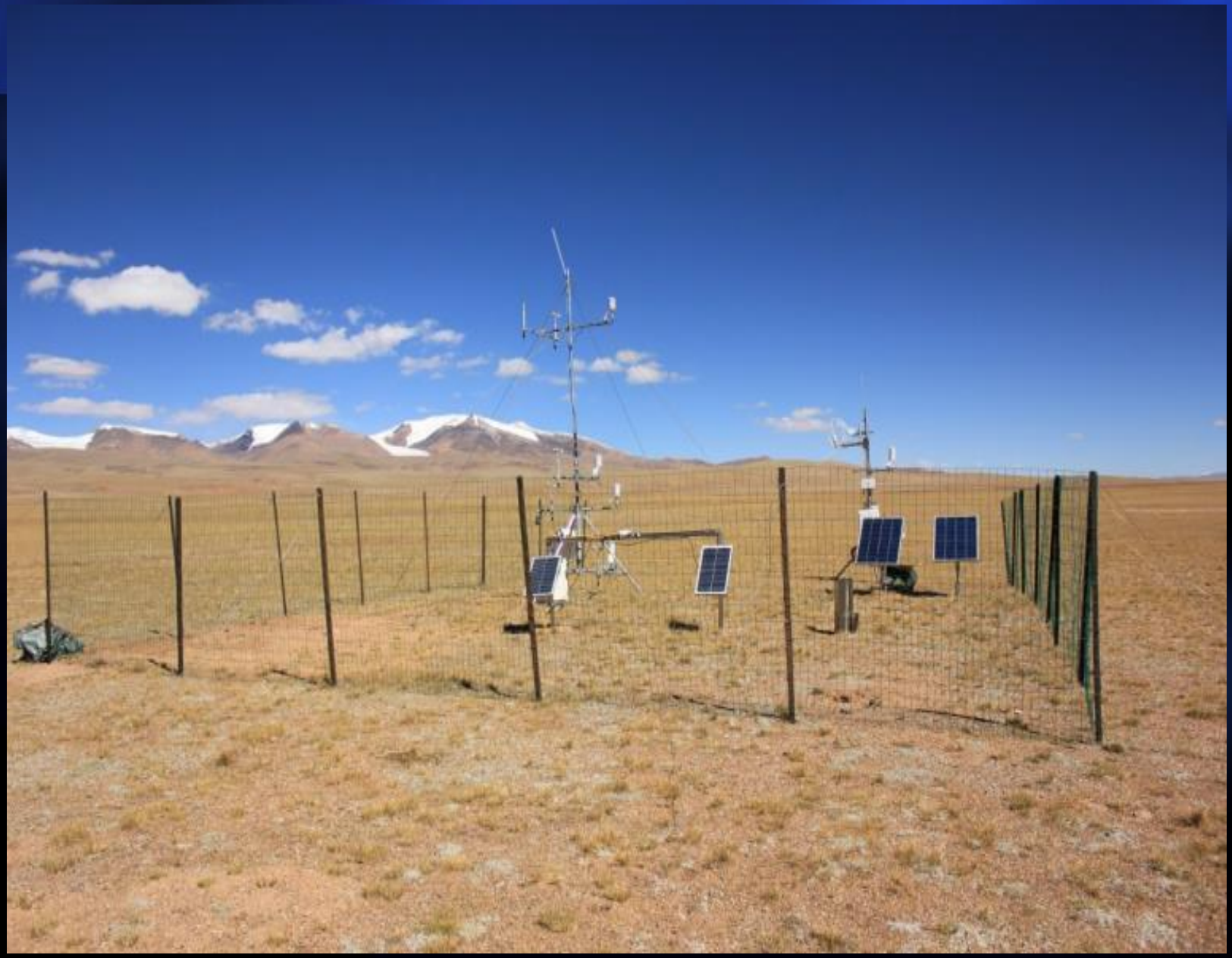

Nagqu Station of Plateau Climate and Environment (NPCE)

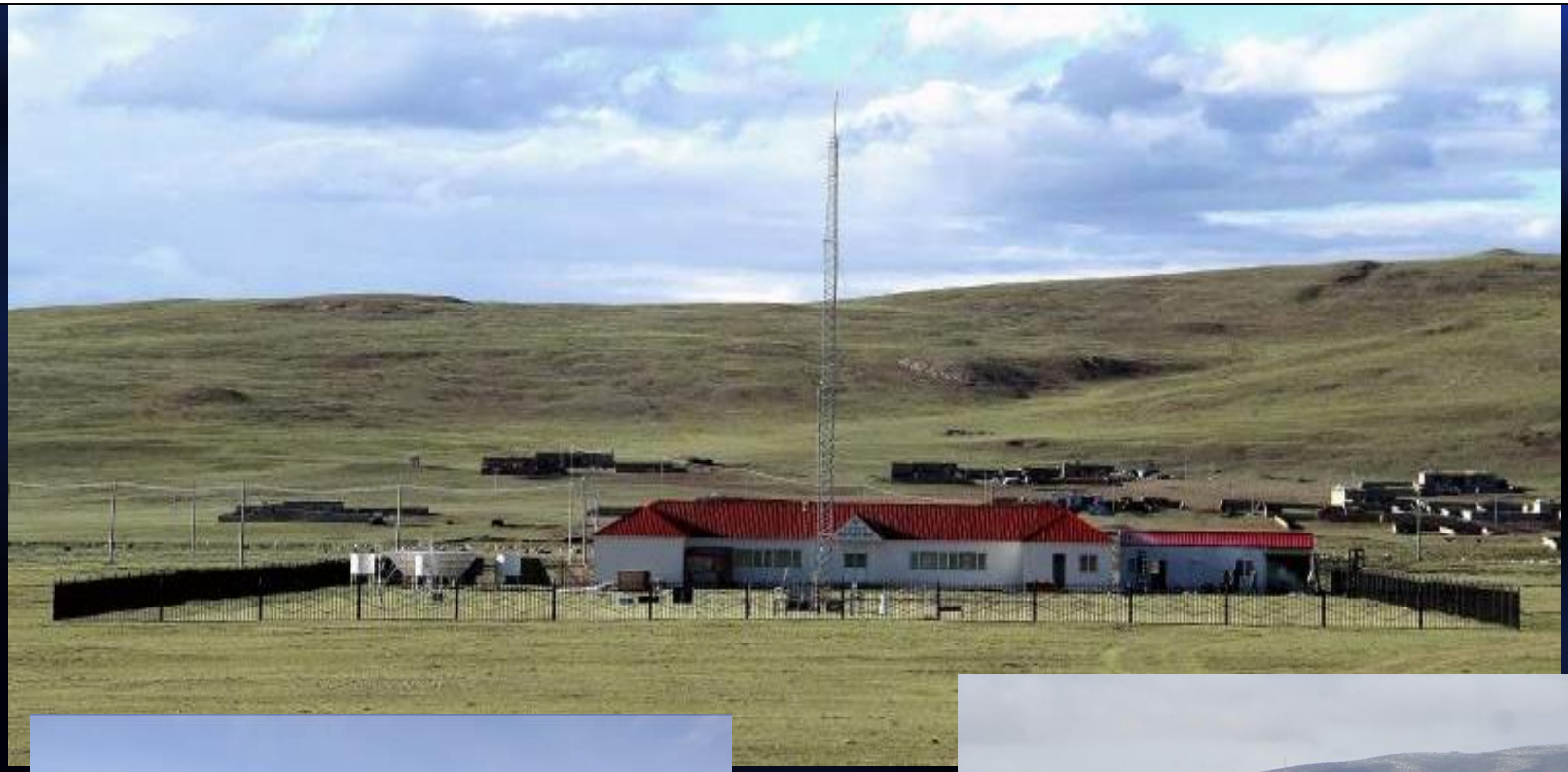

Results from the field observations

•*The eddy correlation methodology*

Momentum flux $\tau = -\rho\overline{u'w'} = \rho u_*^{\,2}$

Sensible heat flux $H = \rho C_P \overline{w'T'} = -\rho C_P u_* T_*$

Latent heat flux $\lambda E = \lambda\rho\overline{w'q'} = -\lambda\rho u_* q_*$

Friction velocity $u_* = \sqrt{\left|-\overline{u'w'}\right|}$

Characteristic temperature $T_* = -\dfrac{\overline{w'T'}}{u_*}$

Characteristic specific humidity $q_* = -\dfrac{\overline{w'q'}}{u_*}$

Stability parameter $\zeta = z/L = -\dfrac{zTu_*^{\,3}}{kg\overline{w'T'}} = -\dfrac{zTu_*^{\,3}\rho C_P}{kgH}$

•The Bowen ratio methodology

momentum flux $\tau = \rho C_{DN}(u_z - u_s)^2$

sensible heat flux $H = \rho C_p C_{HN}(u_z - u_s)\left(T_{sfc} - T_z\right)$

latent heat flux $\lambda E = \rho \lambda C_{EN}(u_z - u_s)\left(q_{sfc} - q_z\right) = H \cdot B^{-1}$

Bowen ratio $B = \dfrac{C_p(T_{z_1} - T_{z_2})}{\lambda(q_{z_1} - q_{z_2})} = \dfrac{H}{\lambda E}$

$$C_{DN} = \frac{k^2}{[\ln(z/z_0)]^2} = -\frac{\overline{u'w'}}{U^2}$$

$$C_{HN} = -\frac{\overline{w'T'}}{U(T_s - T_a)}$$

•*Micrometeorological characteristics parameters*

Aerodynamic roughness length z_{0m}

$$z_{0m} = ze^{-\frac{kU}{u_*}-\psi_m(\frac{z}{L})}, \qquad z_{0m} = e^{(\frac{U_2 \ln z_1 - U_1 \ln z_2}{U_2 - U_1})}$$

Thermodynamic roughness length

$$z_{0h} = ze^{-\frac{k(T-T_s)}{T_s}-\psi_h(\frac{z}{L})}$$

Excess resistance to heat transfer kB^{-1}

$$kB^{-1} = \ln(\frac{z_{om}}{z_{0h}}), \qquad kB^{-1} = \frac{ku_*(T_s - T)}{H_{obs}/\rho C_P} - [\ln\frac{z-d_0}{z_{0m}} - \psi_h(\frac{z}{L})]$$

GAME/Tibet

R_n: Net radiation
H: Sensible heat flux
LE:Latent heat flux
G_0: Soil heat flux

2.1 "Surface energy imbalance"(PAM data)

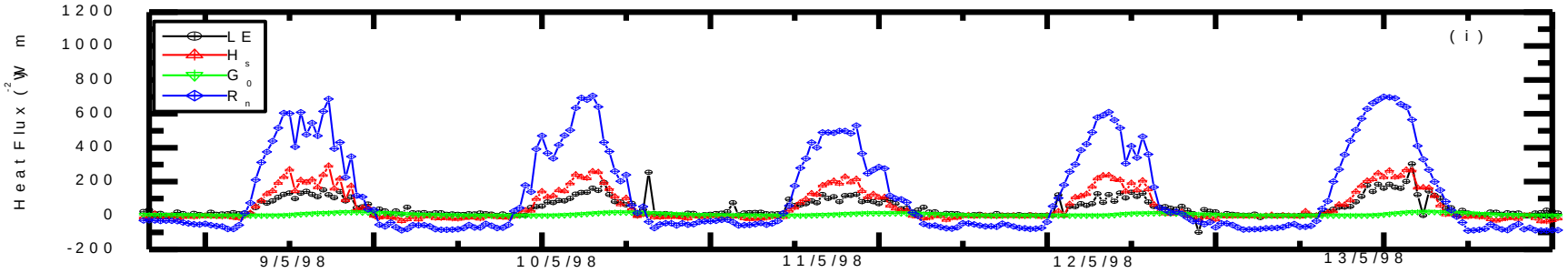

Sensible heat flux and latent heat flux by using **sonic-anemometer data**

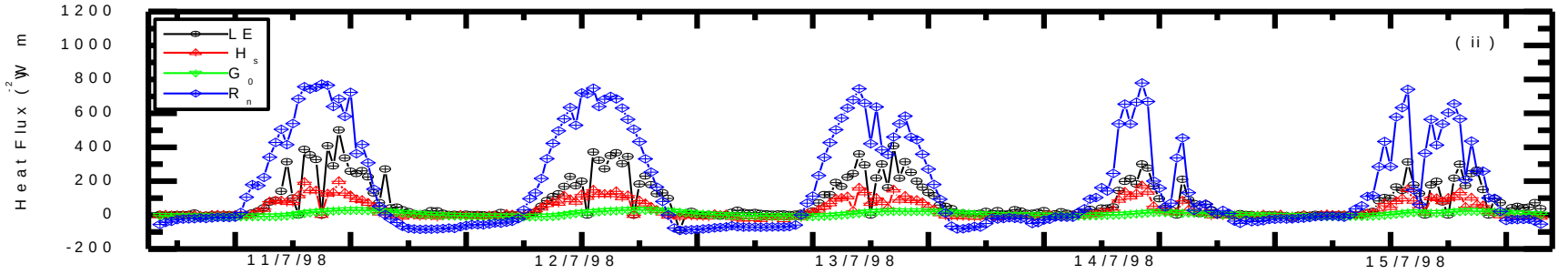

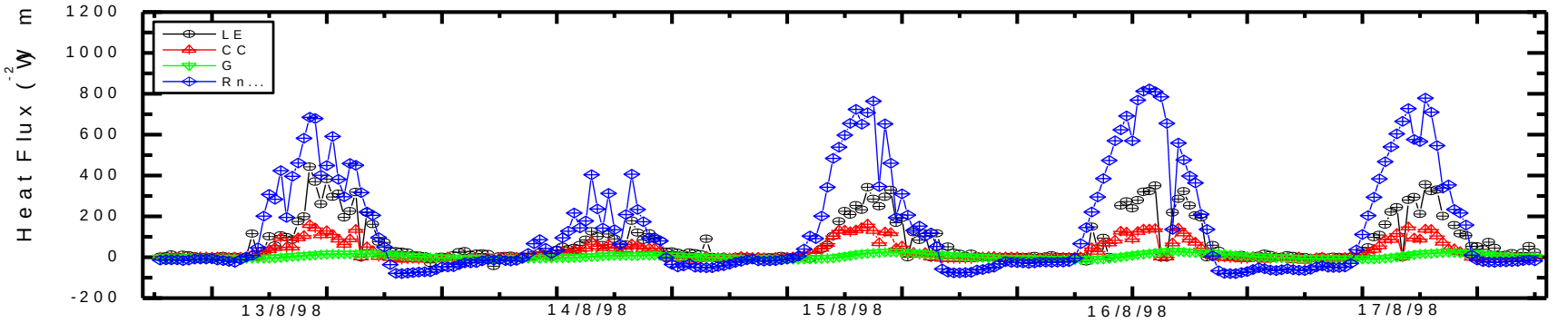

Land surface heat fluxes

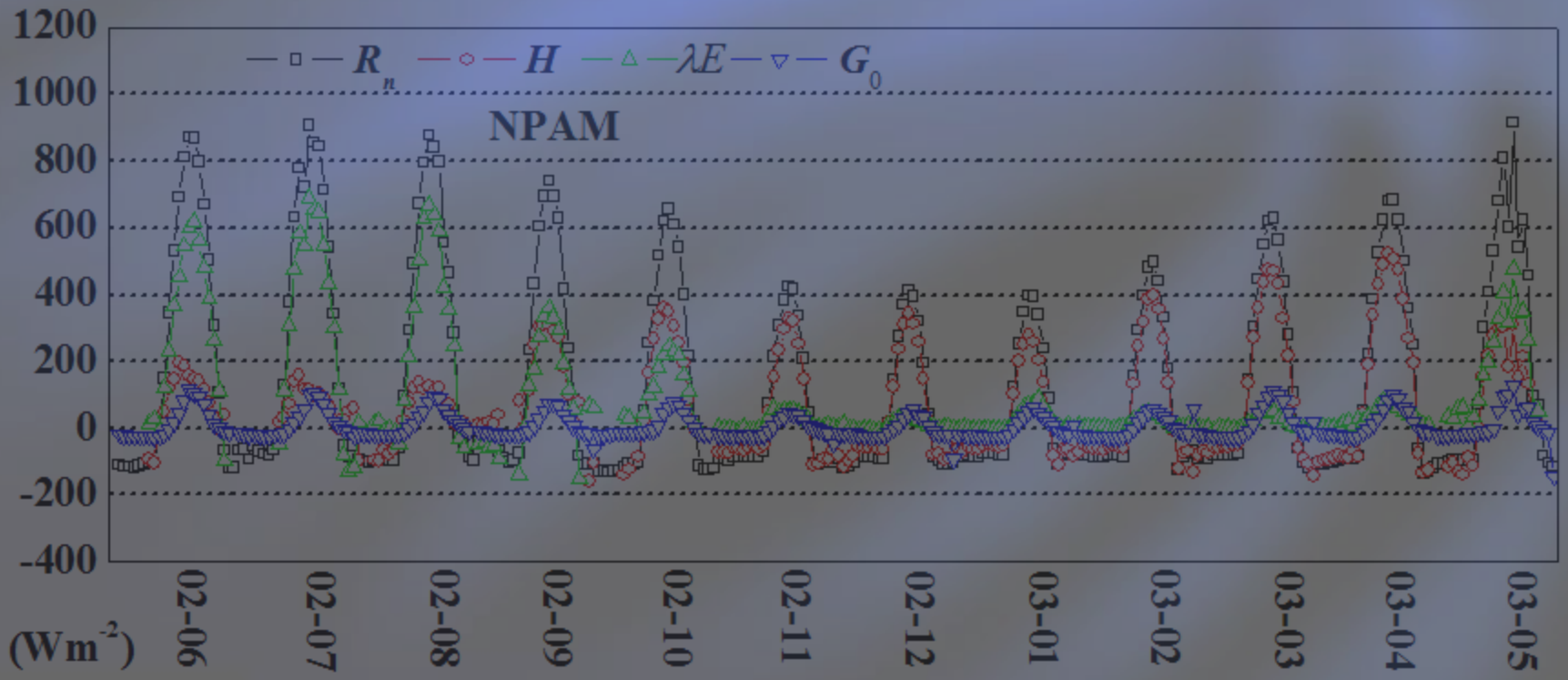

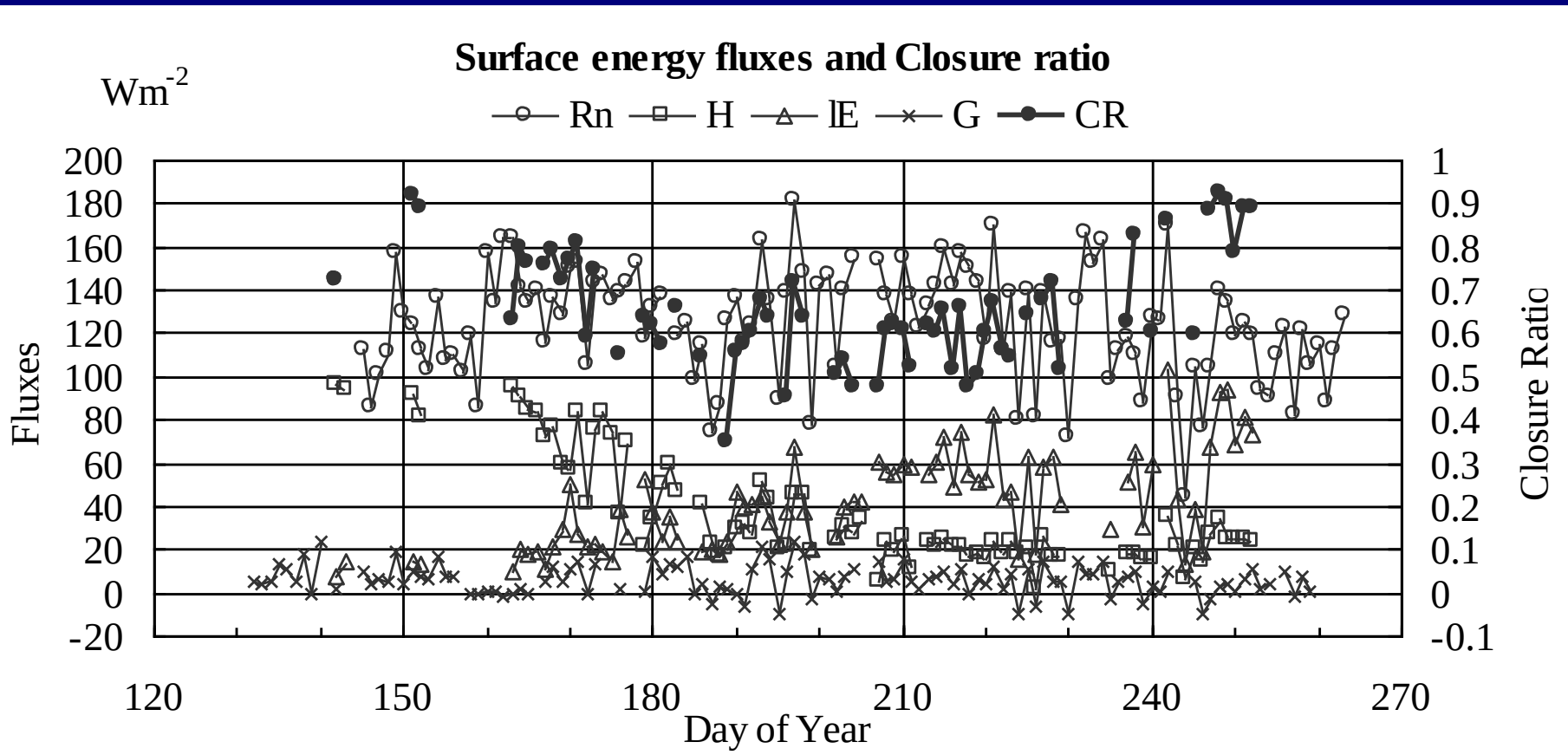

Daily averaged surface energy fluxes and its closure ratio (CR) during IOP (Tanaka et al.,2003)

Sensible heat flux and latent heat flux by using PBL tower data (one year analysis)

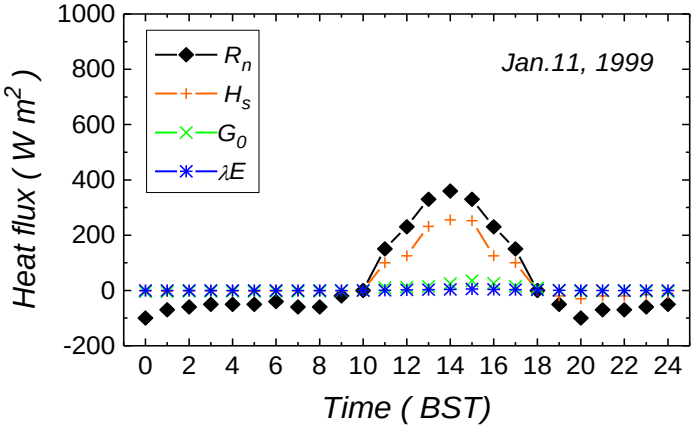

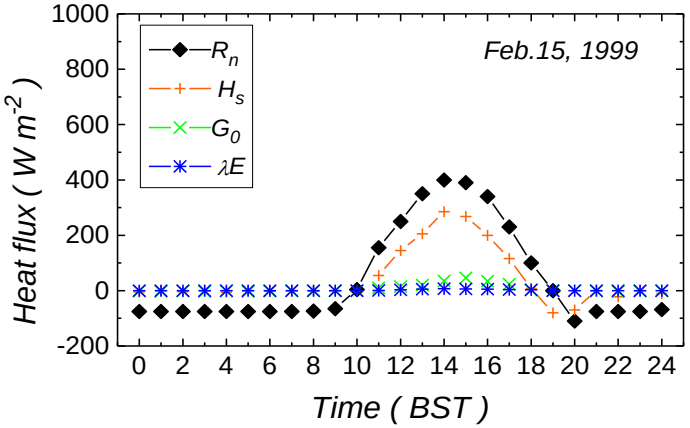

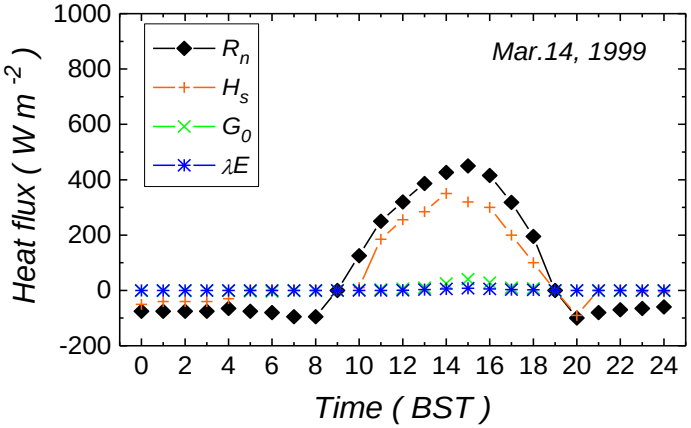

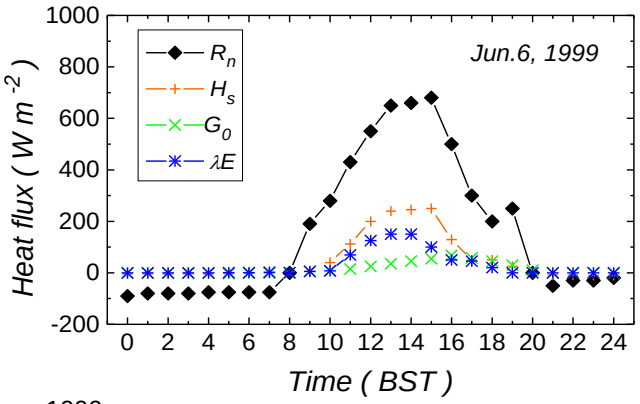

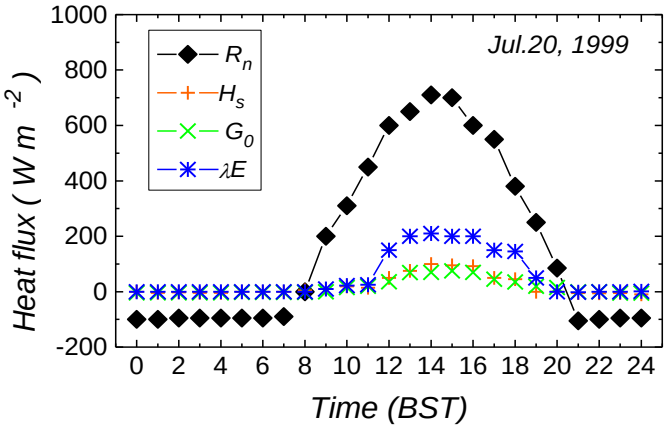

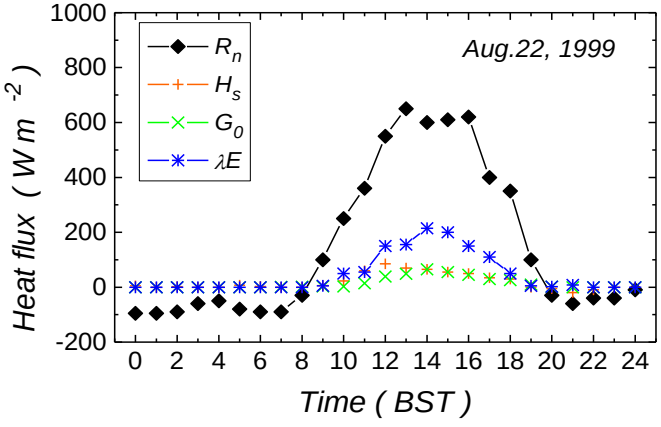

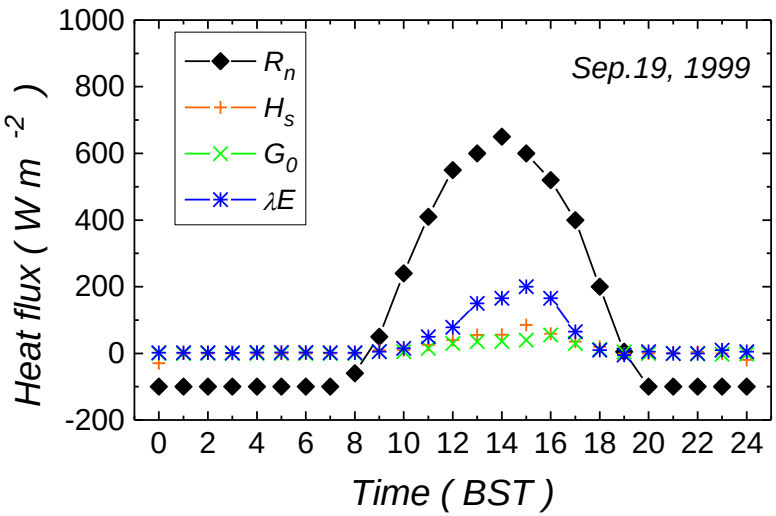
Sep.19, 1999
R_n
H_s
G_0
λE
Heat flux (W m $^{-2}$)
Time (BST)
1000
800
600
400
200
0
-200
0 2 4 6 8 10 12 14 16 18 20 22 24

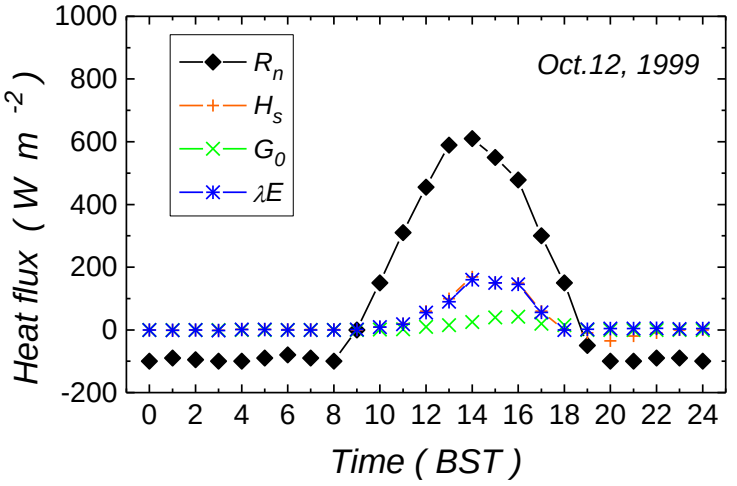
Oct.12, 1999
R_n
H_s
G_0
λE
Heat flux (W m $^{-2}$)
Time (BST)
1000
800
600
400
200
0
-200
0 2 4 6 8 10 12 14 16 18 20 22 24

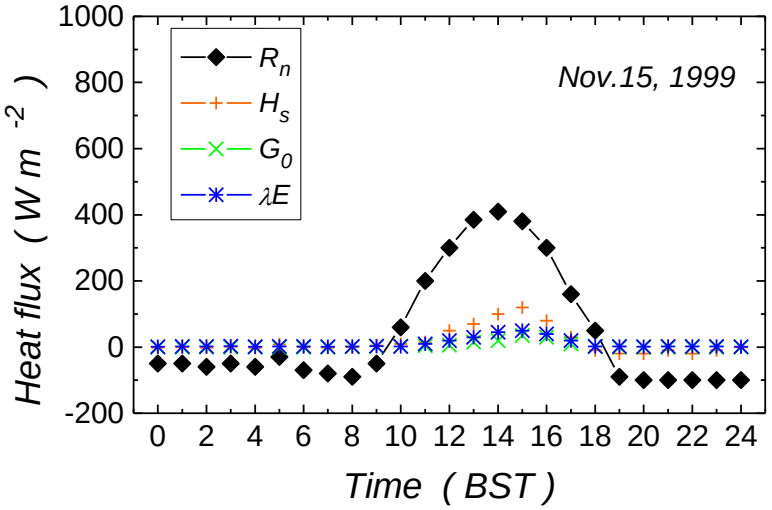
Nov.15, 1999
R_n
H_s
G_0
λE
Heat flux (W m $^{-2}$)
Time (BST)
1000
800
600
400
200
0
-200
0 2 4 6 8 10 12 14 16 18 20 22 24

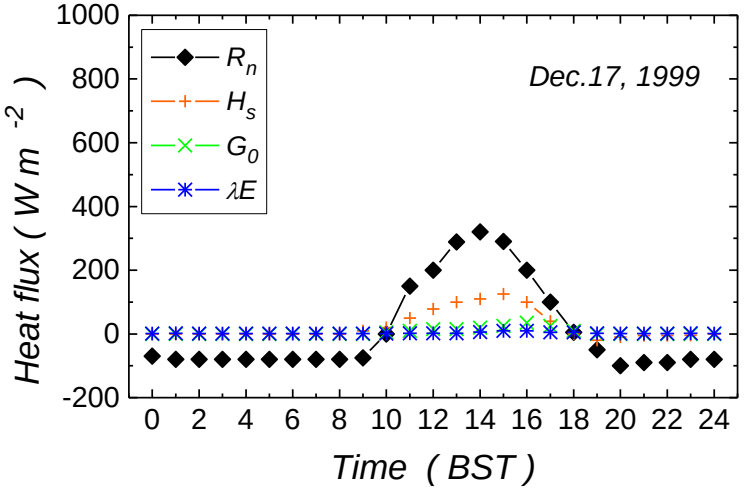
Dec.17, 1999
R_n
H_s
G_0
λE
Heat flux (W m $^{-2}$)
Time (BST)
1000
800
600
400
200
0
-200
0 2 4 6 8 10 12 14 16 18 20 22 24

1. The diurnal variations for surface heat fluxes in the Tibetan Plateau area are very clear;

2. The surface energy budget was, however, not well closed from the observed data. CR=(H+LE)/(Rn-G), the present results shows average CR~0.7(sometimes around 0.9 during the pre-monsoon period), and CR is between 0.5 and 0.7 during the summer monsoon period. And the “imbalance” is more large in summer than it in winter;

Possibilities

1)instruments problems(*LE)*

2) advections around the experimental stations;

3)there exists a discussion that a very weak systematic vertical flow can cause such an imbalance(Lee, 1998)

Further systematic research is necessary to figure out the cause of surface flux imbalances in this area

Radiation

By using the data of D105, Anduo, MS3478(NPAM)and BJ

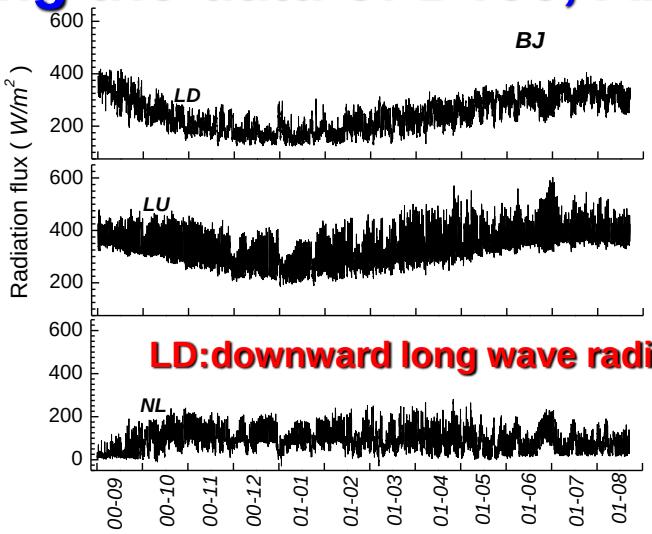

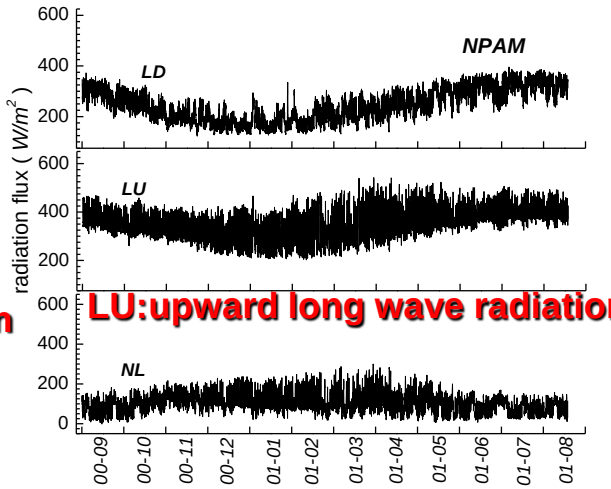

LD:downward long wave radiation

LU:upward long wave radiation

NL:Net long wave radiation

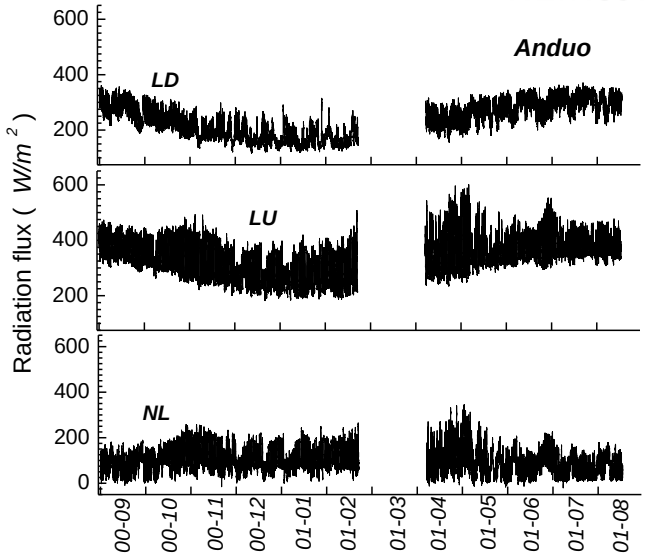

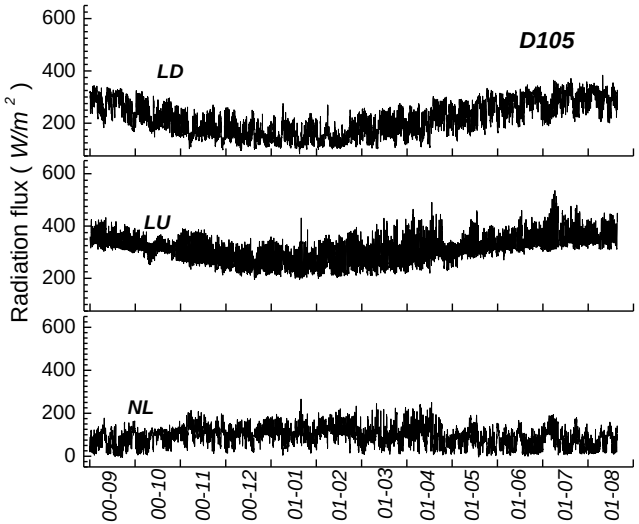

The inter-monthly change of **long-wave radiation** in Tibetan Plateau area

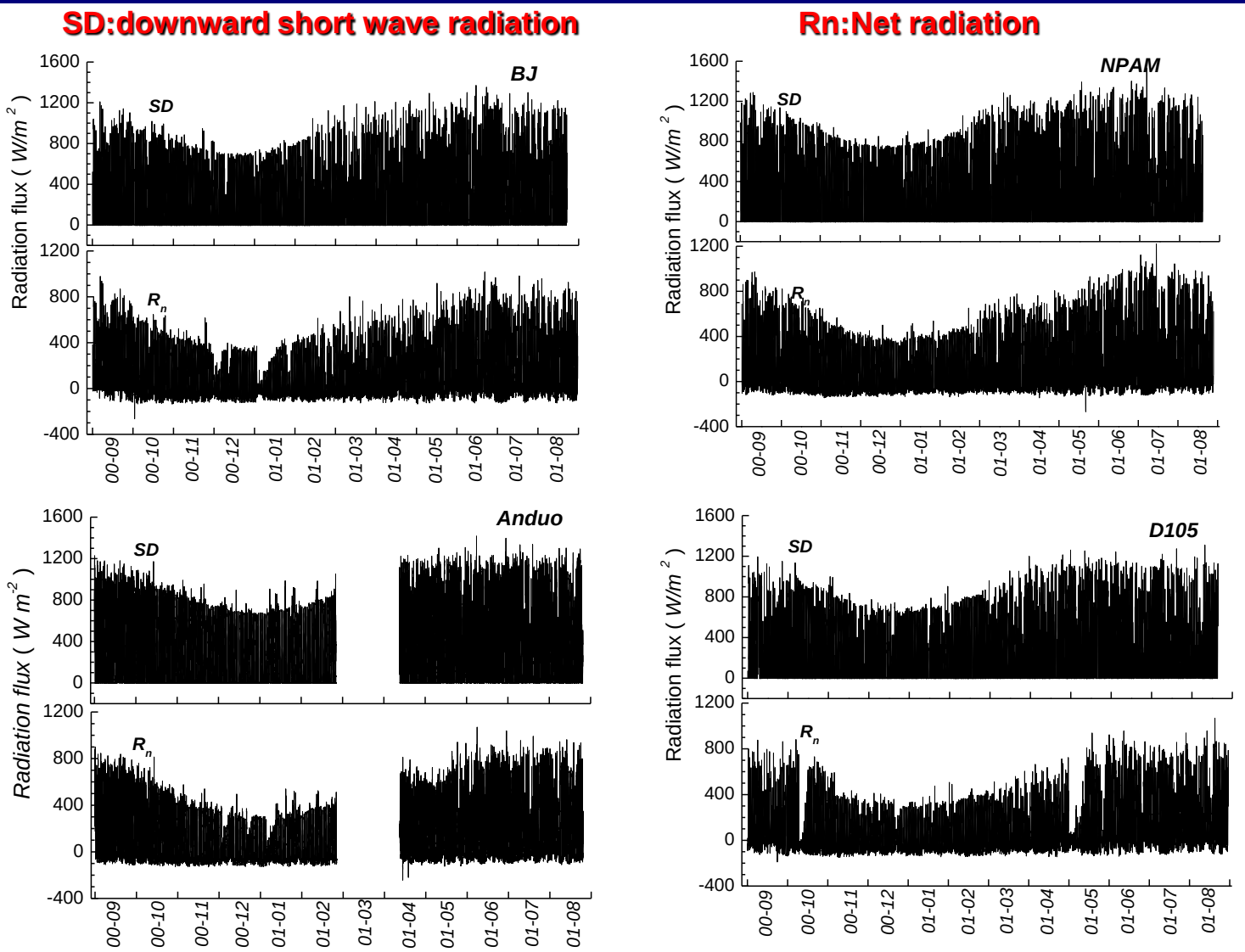

The inter-monthly changes of global radiation and net radiation in Tibetan Plateau area

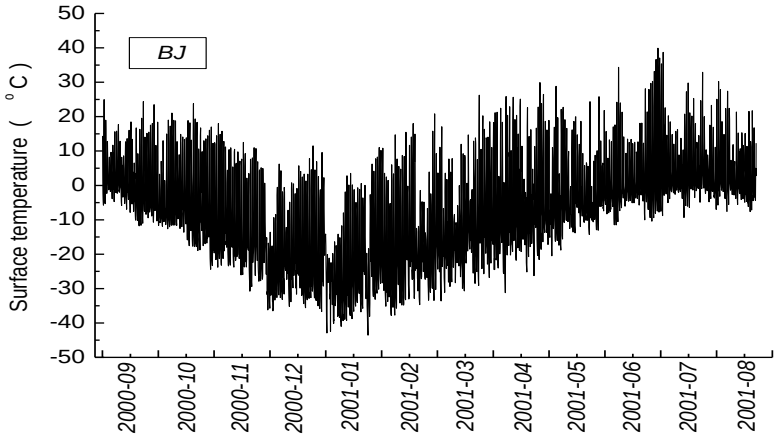

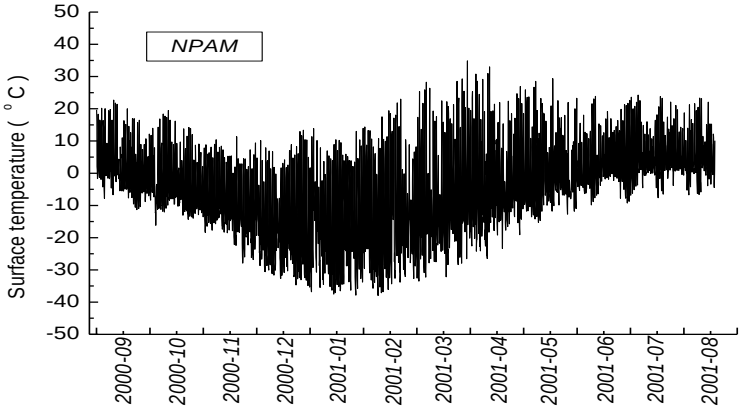

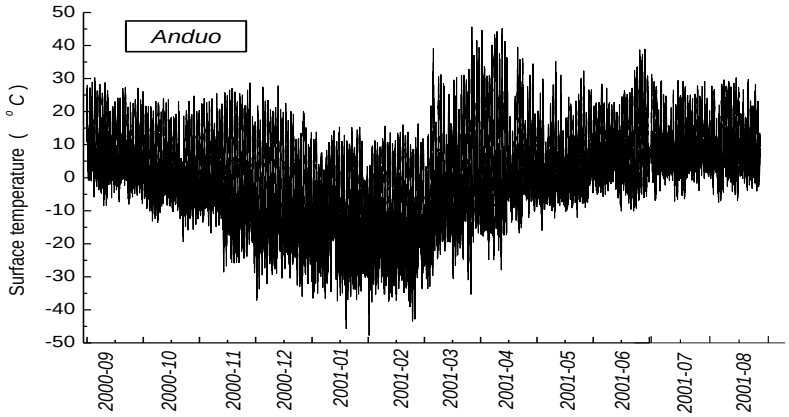

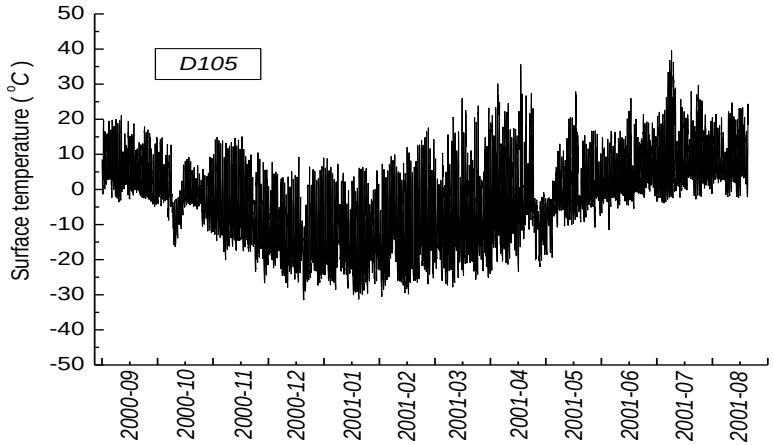

The inter-monthly change of **surface temperature** in Tibetan Plateau area

1. **The inter-monthly variations** of the downward short wave radiation, downward long wave radiation, the upward long wave radiation, net radiation and surface temperature were very obvious. The summer values are larger than it in winter, and they reach the minim value around January;
2. The downward short wave radiation(***SD***) reaches about **1100W/m2** at local noon on fine days in summer. The transmission rate of incoming solar radiation from the top of the atmosphere was estimated as about 85% in cloudless conditions. The values is about 10-15% great than about that observed at the typical sea level station. This is due to the high altitude of the site, thus a shallower atmospheric layer between the top of the atmospheric and the ground surface;
3. The upward long wave , equivalent to the surface temperature.

Aerodynamic and thermodynamic roughness Length

Table 1. Aerodynamic Roughness Length z_{0m} Der… ifferent Land Surfaces by Using the Independent Method

Land surface	Grass land	Grass land	Sand desert	Gobi	bean	wheat	corn
	~5 cm	~15 cm		vegetation (Gobi)			
Observation	2.90	5.60	2.90	2.90	2.90	2.90	4.90
z_{0m}, m	0.00436	0.0139	0.00267	0.0028	0.061	0. 168	0.302

0.0139 (July), 0.0324 (August)

Table 2. Thermodynamic Roughness Length z_{0h} Derived From Different Land Surfaces

	Amdo	*NPAM*	*HEIFE*	*HEIFE*	*HEIFE*	*HEIFE*	*AECMP'95*
Land surface	grassland ~5 cm	grassland ~15 cm	Sand desert	Gobi	bean	wheat	corn
Height of … tation, m							
z_{0h}, m	0.00041	0.00114	0.000049	0.000011	0.000685	0. 00132	0.00227

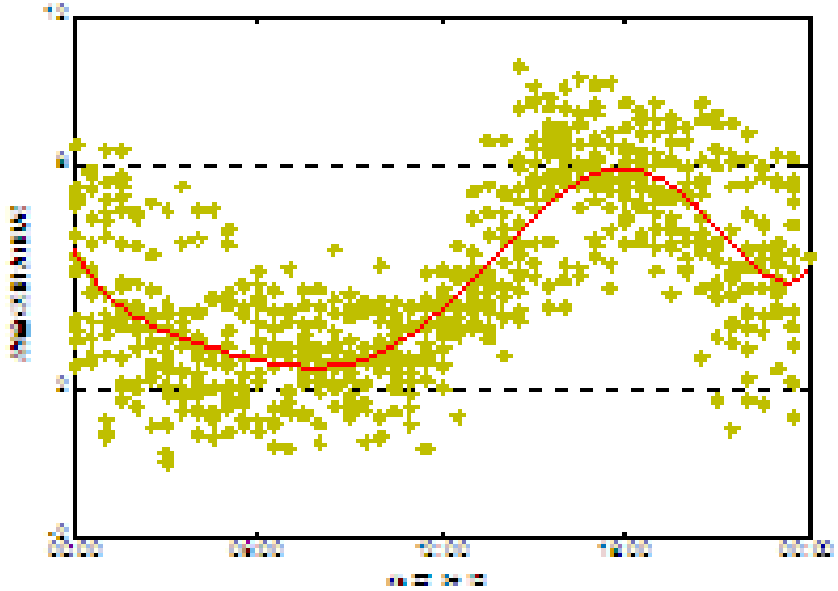

Mt.Everest

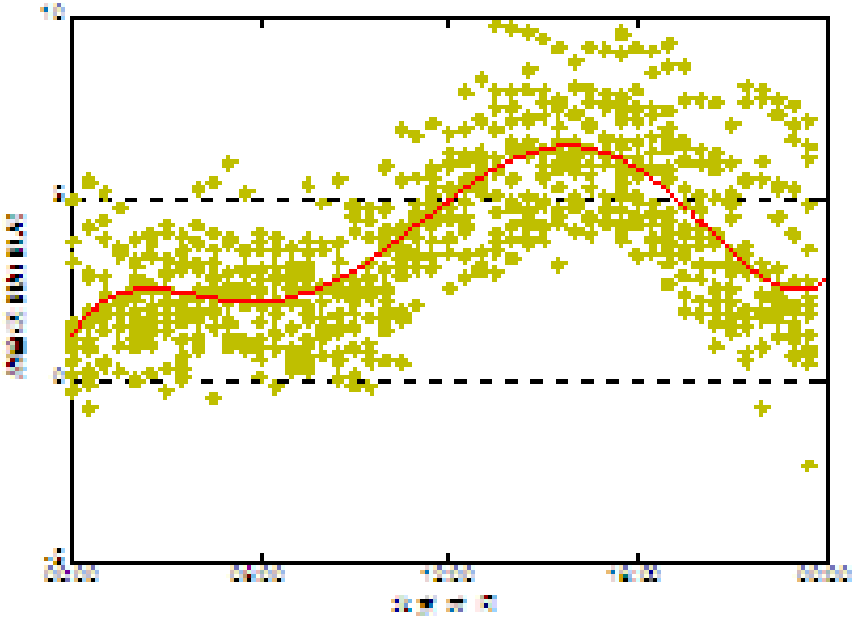

Namco

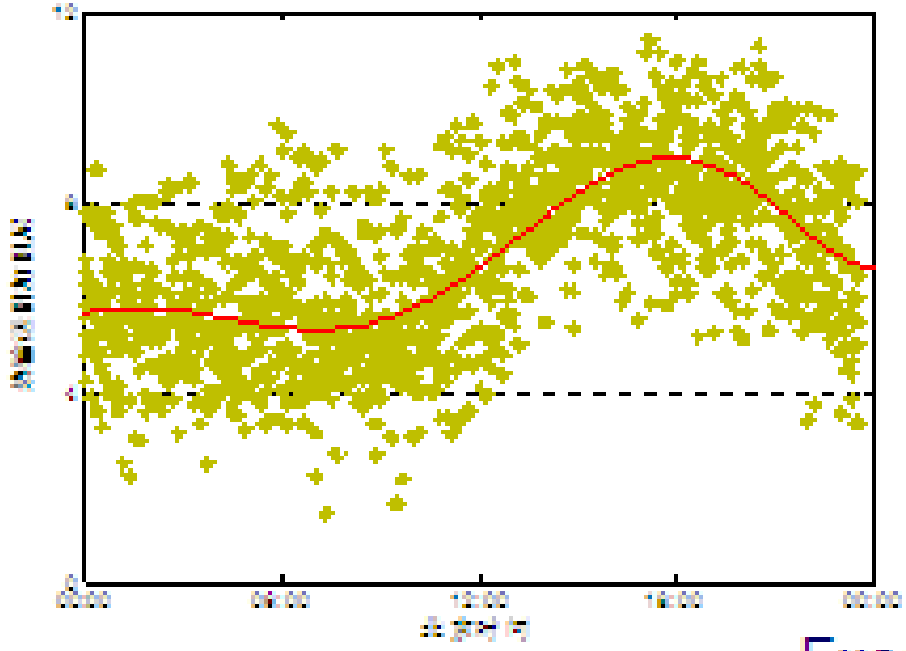

Linzhi

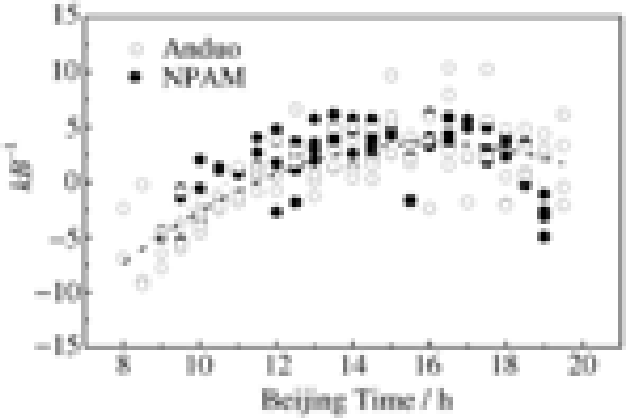

Fig. 2. Diurnal variations of the excess resistance to heat transfer kB^{-1} of Anduo Station and NPAM Station.

Excess resistance to heat transfer (kB-1)

Effective aerodynamic roughness length and zero-plane displacement height

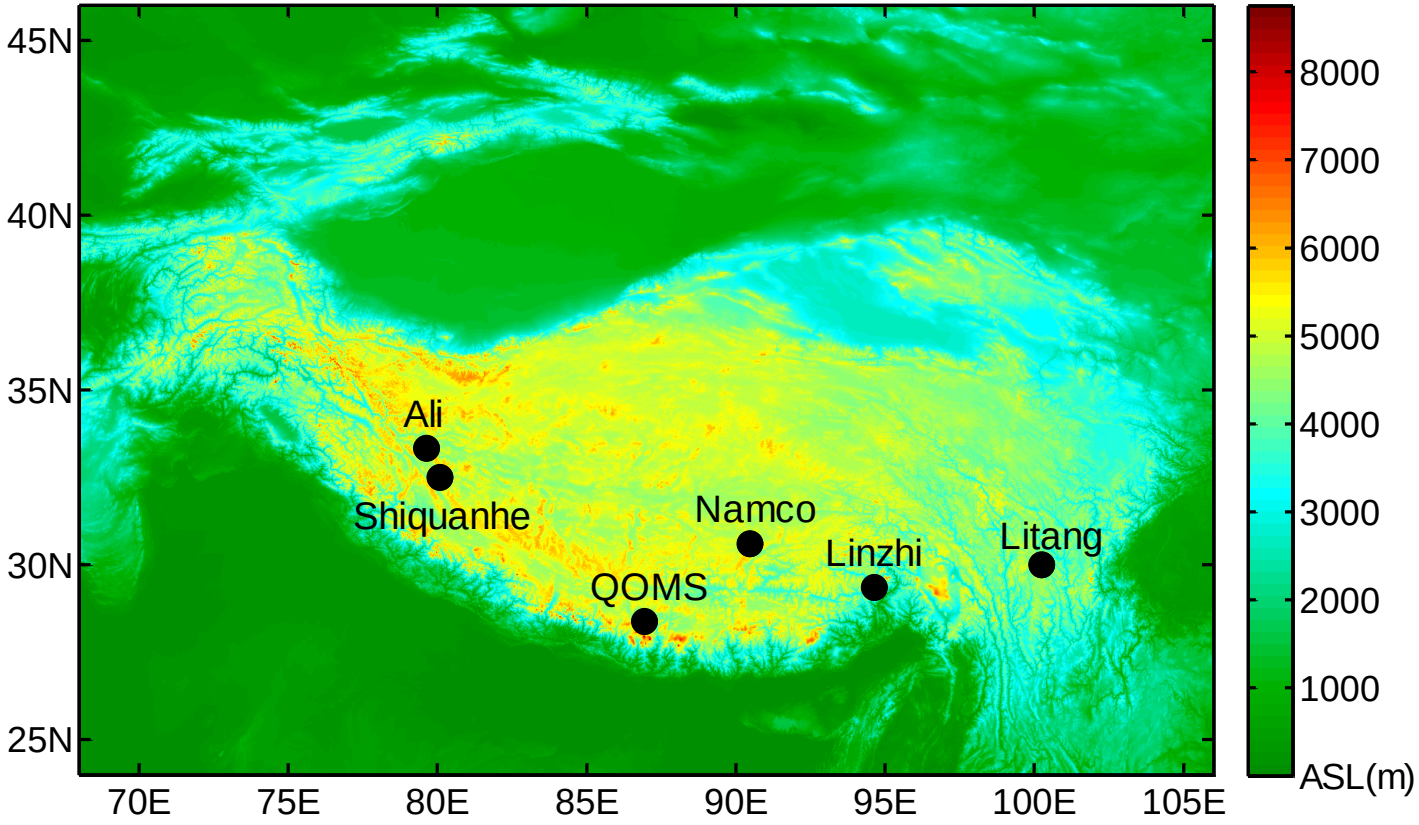

Radio-sonde data ,Wind Profiler data and turbulent data

Radio-sonde and Wind profiler and RASS

Effective aerodynamic roughness length and zero-plane displacement height （Han and Ma et al., 2015,QJRMS)

Station	z_{0m}^{eff} (m)	d_0 (m)
QOMS(15)	62.6 ± 12.3	470.3 ± 48.0
NAMOS(8)	1.7 ± 1.1	19.4 ± 11.9
Linzhi(14)	86.0 ± 6.6	516.1 ± 39.7
Ali(11)	1.9 ±1.1	8.1 ± 5.5
Shiquanhe(12)	10.2 ±4.3	81.9 ± 34.5
Litang(9)	6.0 ±1.1	60.7 ±11.1

Latent heat flux(ET)-by eddy covariance system

Pre-monsoon

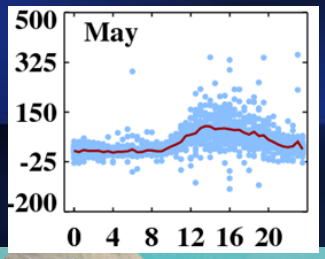

Mustagata Station

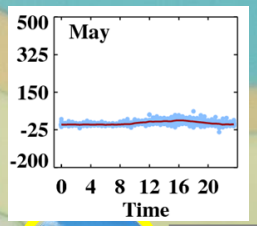

Ali

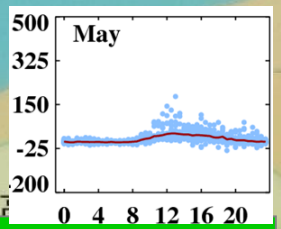

Kekexi

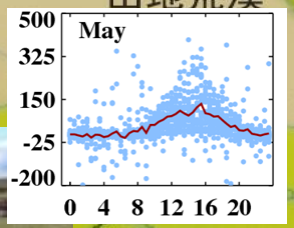

Naqu

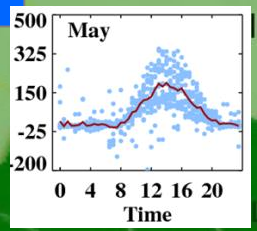

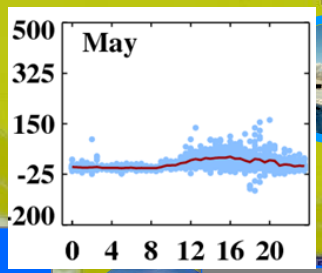

Namco

SETS

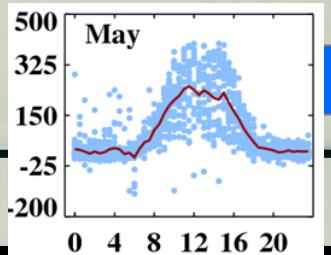

Nepal

QOMS

Yadong

山地荒漠
IID3
山地草原
IIC2
IB1
地
荒
漠
高寒草原
IC2
IID1
山地森林
IIAB1
草原
亚热带山地森林
OA1
0
800 KM

Latent heat flux(ET)-by eddy covariance system

Monsoon

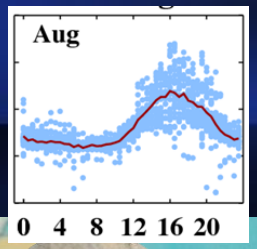

Mustagata Station

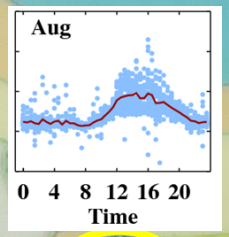

Ali Station

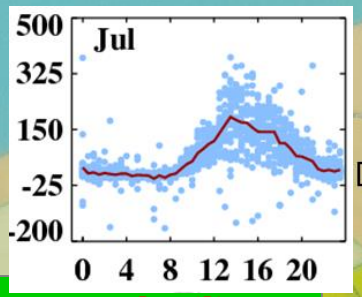

Kekexili

D3

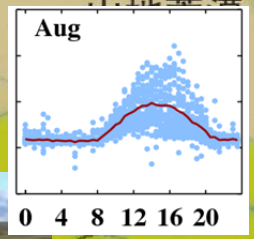

Naqu station

山地草原
IIC2

高寒草甸 IB1

荒
漠

IID1

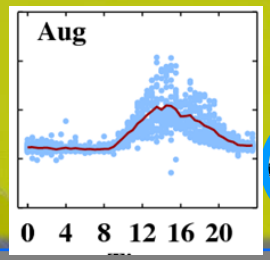

高寒草
IC2

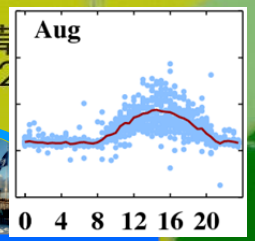

Namco

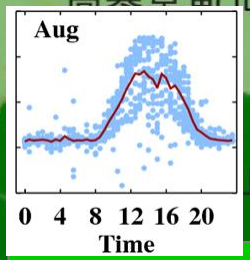

SETS

山地森林
IIAB1

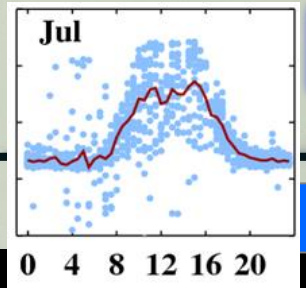

QOMS

0

600 km

地灌丛草原 IIC1

Nepal

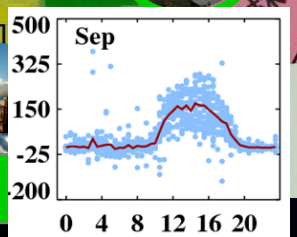

Yadong

A1

Latent heat flux(ET)-by eddy covariance system

Post-monsoon

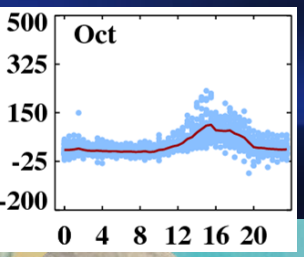

Mustagata Station

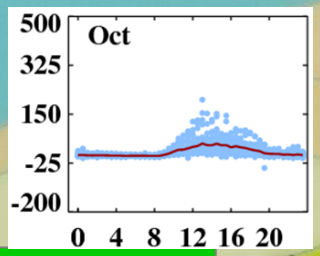

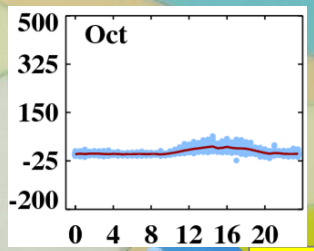

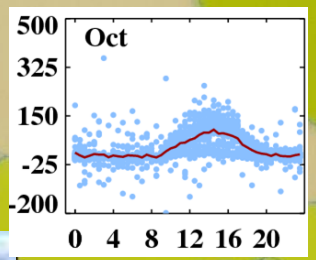

IID3

山地草原
IIC2

Kekexili

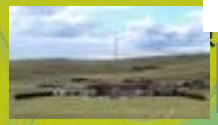

Naqu

Ali

荒
漠

IID1

高寒草
IC2

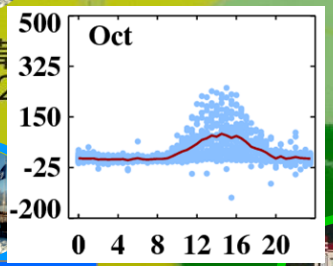

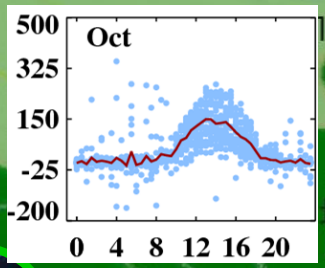

地森林
IIAB1

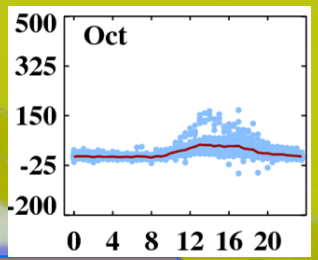

Namco

SETS

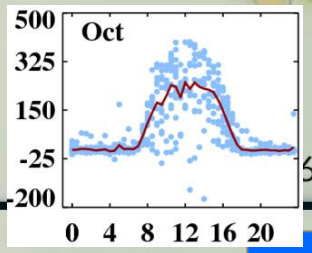

0

600

QOMS

山地灌丛草原 IIC1

Nepal

Yadong

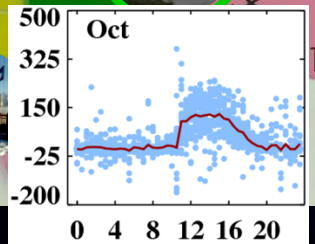

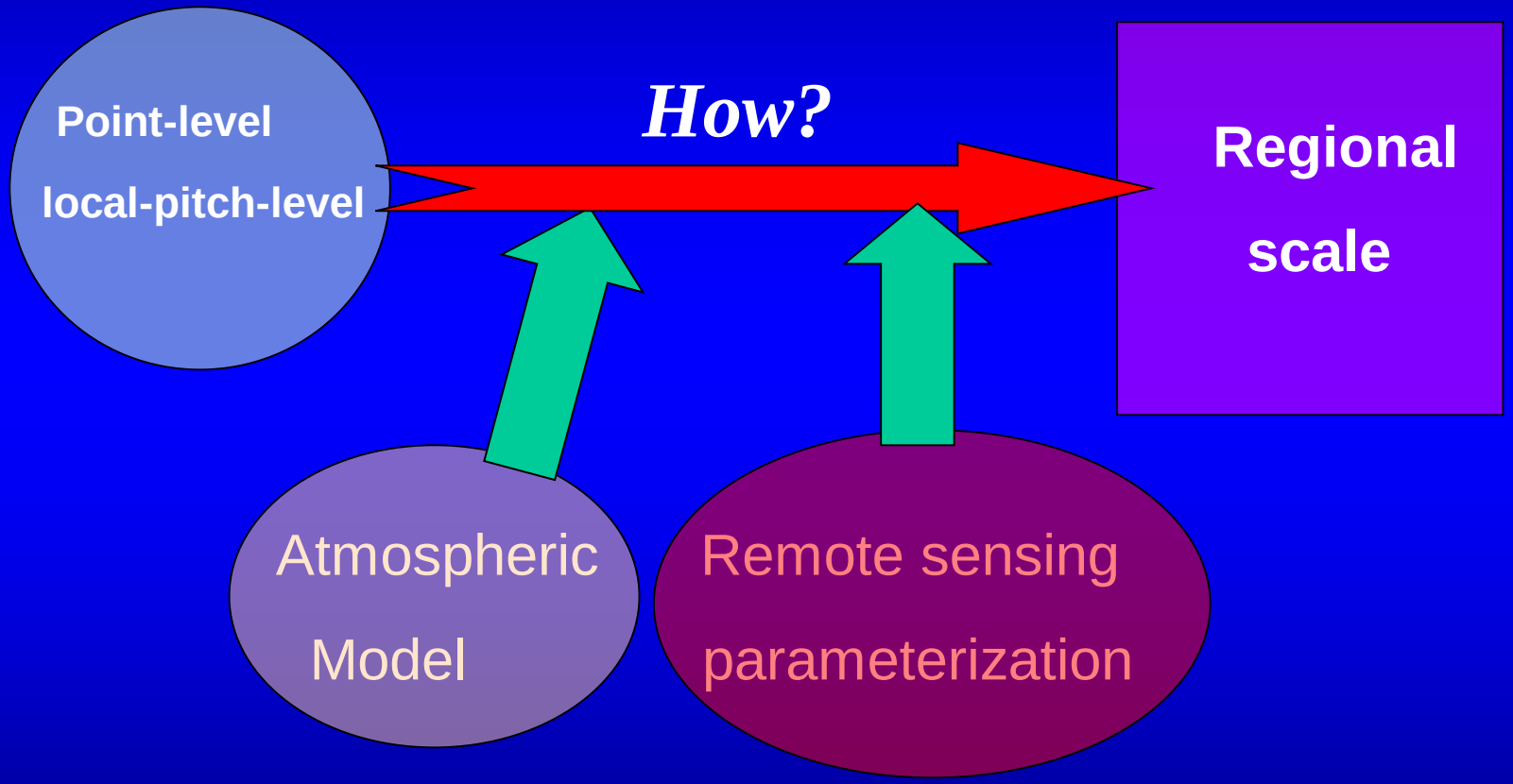
Point-level
local-pitch-level
How?
Regional
scale
Atmospheric
Model
Remote sensing
parameterization

❑Regional Results

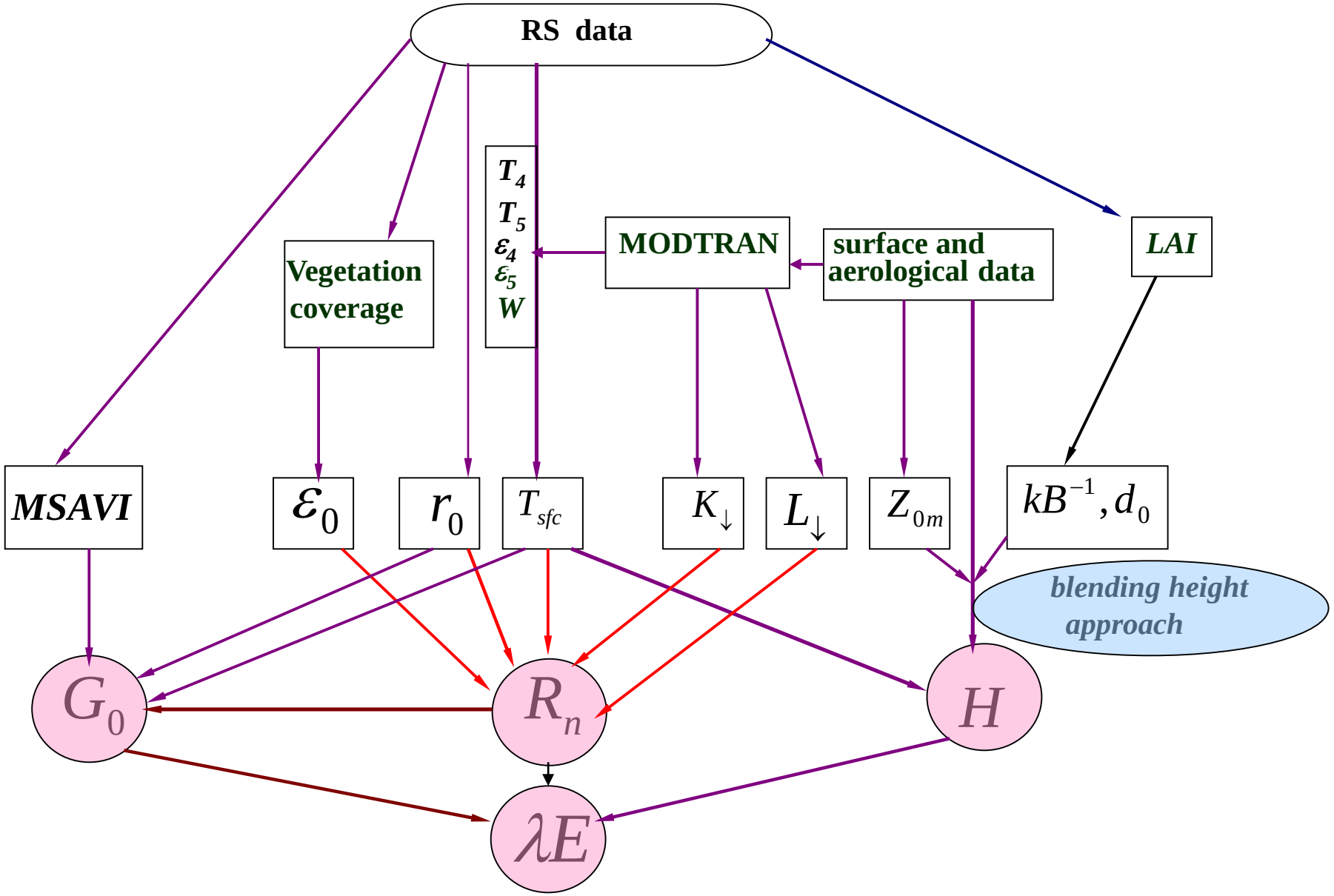

Fig. Diagram of parameterization procedure by combining NOAA AVHRR data with field observations

❖*Surface reflectance (surface albedo)*

Land surface reflectance on each pixel derived from NOAA/AVHRR:

$$r_{broadband}(x,y) = a \cdot r_{AVHHR-1}(x,y) + b \cdot r_{AVHRR-2}(x,y) + c \qquad (1.3)$$

Tibetan Plateau:

$$r_{broadband}(x,y) = 0.546 r_{AVHHR-1}(x,y) + 0.454 r_{AVHRR-2}(x,y) + 0.038 \qquad (1.4)$$

❖Surface temperature

Split-window technique (SWT) was proposed (Becker and Li 1990, Becker and Li 1995, Sobrino *et al.* 1994, Sobrino *et al.* 2000):

$$T_{sfc} = A_0 + A_1 T_i + A_2 T_j \qquad (1.5)$$

$$T_{sfc} = F(T_4, T_5, \varepsilon_4, \varepsilon_5, W, \theta) \qquad (1.6)$$

where T_4 and T_5 : the brightness temperatures of channel 4 and 5 of AVHRR;
ε_4 and ε_5 : the spectral emissivities of channel 4 and 5 respectively;
W: water vapor content, and θ: the view angle from satellite

Equation(1.6) different form by more than 15 researchers , we derived it for

Tibetan Plateau as

$$T_{sfc}(x,y) = T_4(x,y) + 1.56[T_4(x,y) - T_5(x,y)] + 0.28[T_4(x,y) - T_5(x,y)]^2 + (48 - 5W)[1 - \varepsilon(x,y)] \qquad (1.7)$$

where W can be derived from radiation transfer model MODTRAN; ε(x,y)is a function of vegetation coverage

$$\varepsilon(x,y) = \underbrace{\varepsilon_v(x,y)P_v(x,y)}_{\text{Vegetation}} + \underbrace{\varepsilon_g(x,y)(1 - P_v(x,y))}_{\text{Soil}} + 4 < \varepsilon > (1 - P_v(x,y))P_v(x,y) \qquad (1.8)$$

•Normalized Difference Vegetation Index (*NDVI*)

Normal: $NDVI = \frac{r_{nir} - r_{vis}}{r_{nir} + r_{vis}}$

Landsat TM

$$NDVI(x,y) = \frac{r_4(x,y) - r_3(x,y)}{r_4(x,y) + r_3(x,y)}$$

•Modified Soil Adjusted Vegetation Index (*MSAVI*).

Problems exist in the NDVI definition equation because of the external factor effect, such as soil back ground variations (Huete *et al*. 1985, Huete 1989). To reduce the soil back ground effect, MSAVI was proposed(Qi et al, 1994):

$$MSAVI = \frac{2r_{NIR} + 1 - \sqrt{[2r_{NIR} + 1]^2 - 8[r_{NIR} - r_{RED}]}}{2} \qquad (17)$$

Landsat TM

$$MSAVI(x,y) = \frac{2r_4(x,y) + 1 - \sqrt{[2r_4(x,y) + 1]^2 - 8[r_4(x,y) - r_3(x,y)]}}{2}$$

- **Vegetation coverage *Pv***

Carlson and Ripley (1997):

$$P_v(x,y) = \left[\frac{NDVI(x,y) - NDVI_{\min}}{NDVI_{\max} - NDVI_{\min}}\right]^2$$

$$LAI(x,y) = -\frac{1}{2k}\ln\left[\frac{r(x,y) - r_v}{r_s - r_v}\right]$$

This Equation can be used to most of the satellite, such as NOAA/AVHRR, Landsat TM etc.

2 .Land surface heat fluxes

- Net radiation

$$R_n(x,y) = (1 - r_0(x,y)) \bullet K_{\downarrow}(x,y) + L_{\downarrow}(x,y) - \varepsilon_0(x,y)\sigma T_{sfc}{}^4(x,y)$$

•Soil heat flux

$$G_0(x,y) = \rho_s C_s [(T_{sfc}(x,y) - T_s(x,y)] / r_{sh}(x,y)$$

Based on the field observations, we proposed soil heat flux on each pixel as

GAME/Tibet case:

$$G_0(x,y) = R_n(x,y) \frac{T_{sfc}(x,y)}{r_0(x,y)} (0.00025 + 0.00436\,\bar{r}_0 + 0.00845\,\bar{r}_0^{\,2}) \bullet [1 - 0.979\,MSAVI(x,y)^4]$$

- **Sensible heat flux**

$$H(x,y) = \rho C_p k^2 u_B \frac{[T_{sfc}(x,y) - T_a(x,y)]}{[\ln \frac{z_B - d_0(x,y)}{Z'_{0m}(x,y)} + kB^{-1}(x,y) - \psi_h(x,y)] \bullet [\ln \frac{z_B - d_0(x,y)}{Z'_{0m}(x,y)} - \psi_m(x,y)]}$$

❖Latent heat flux

$$\lambda E(x,y) = R_n(x,y) - H(x,y) - G_0(x,y)$$

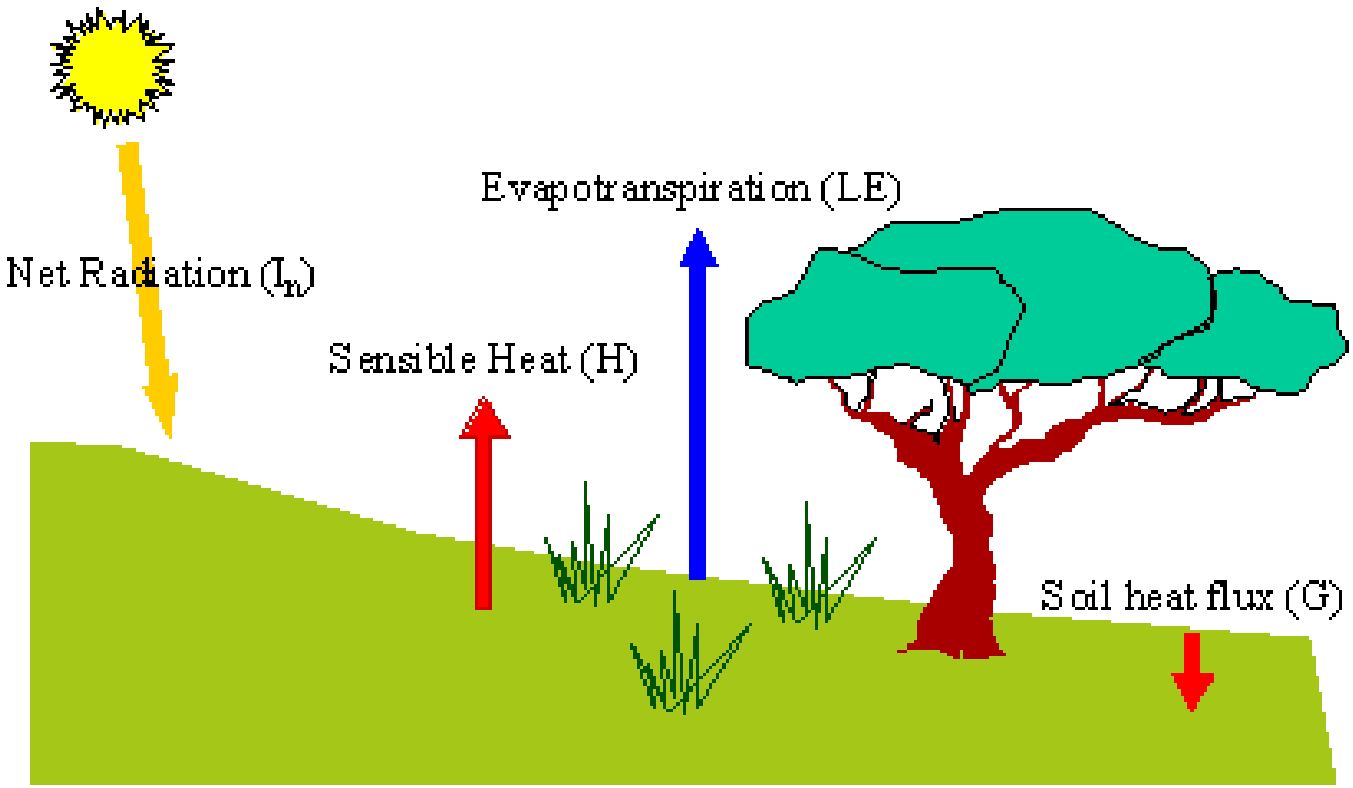

Case study

The scene of June 12, 1998 is selected as a case of pre-monsoon and whole meso-scale area. The scenes of July 16, 1998 and August 21, 1998 are selected as the cases of mid-monsoon and the post-monsoon.

NDVI ***MSAVI***

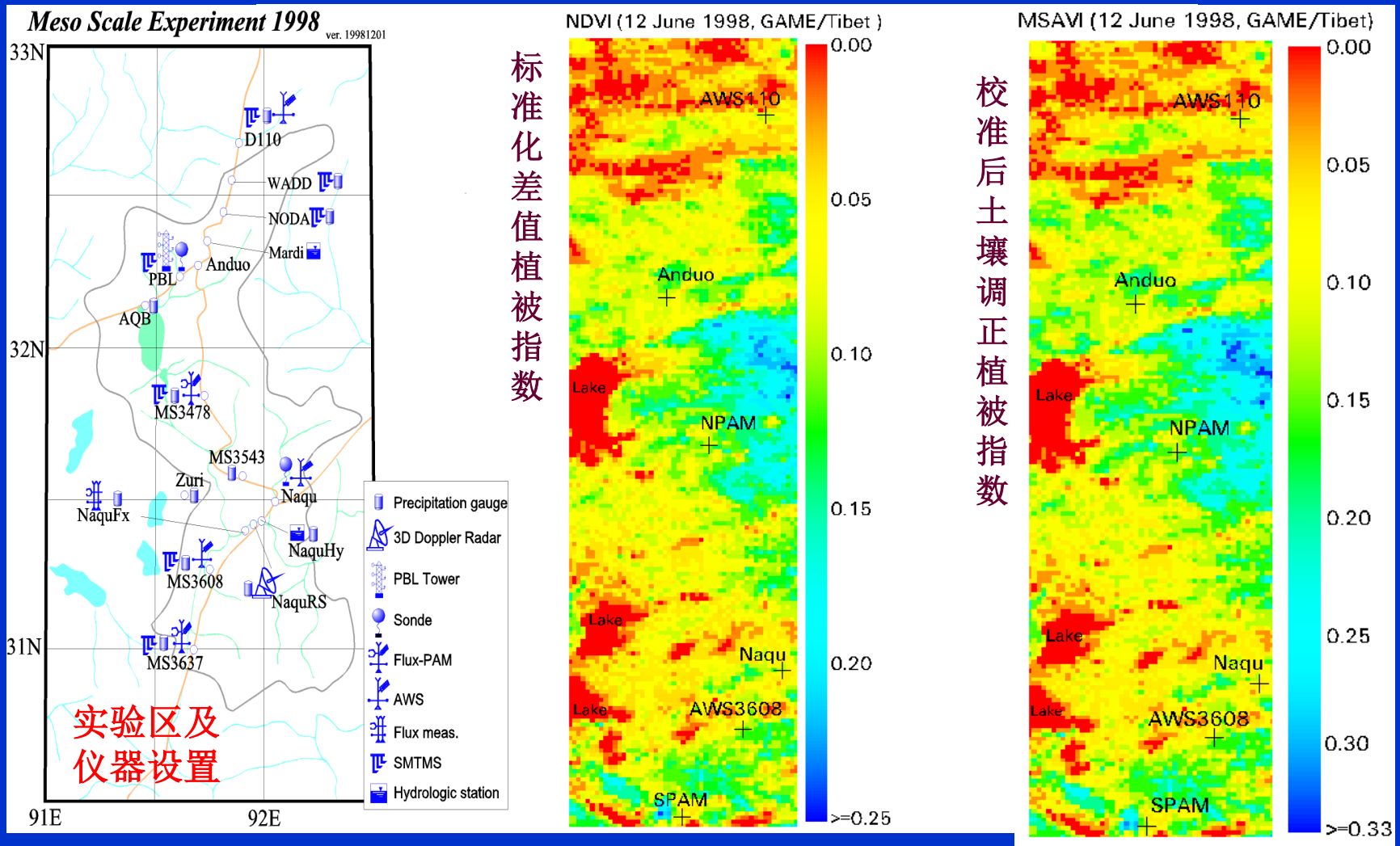

Vegetation coverage

LAI

Surface reflectance

Surface temperature

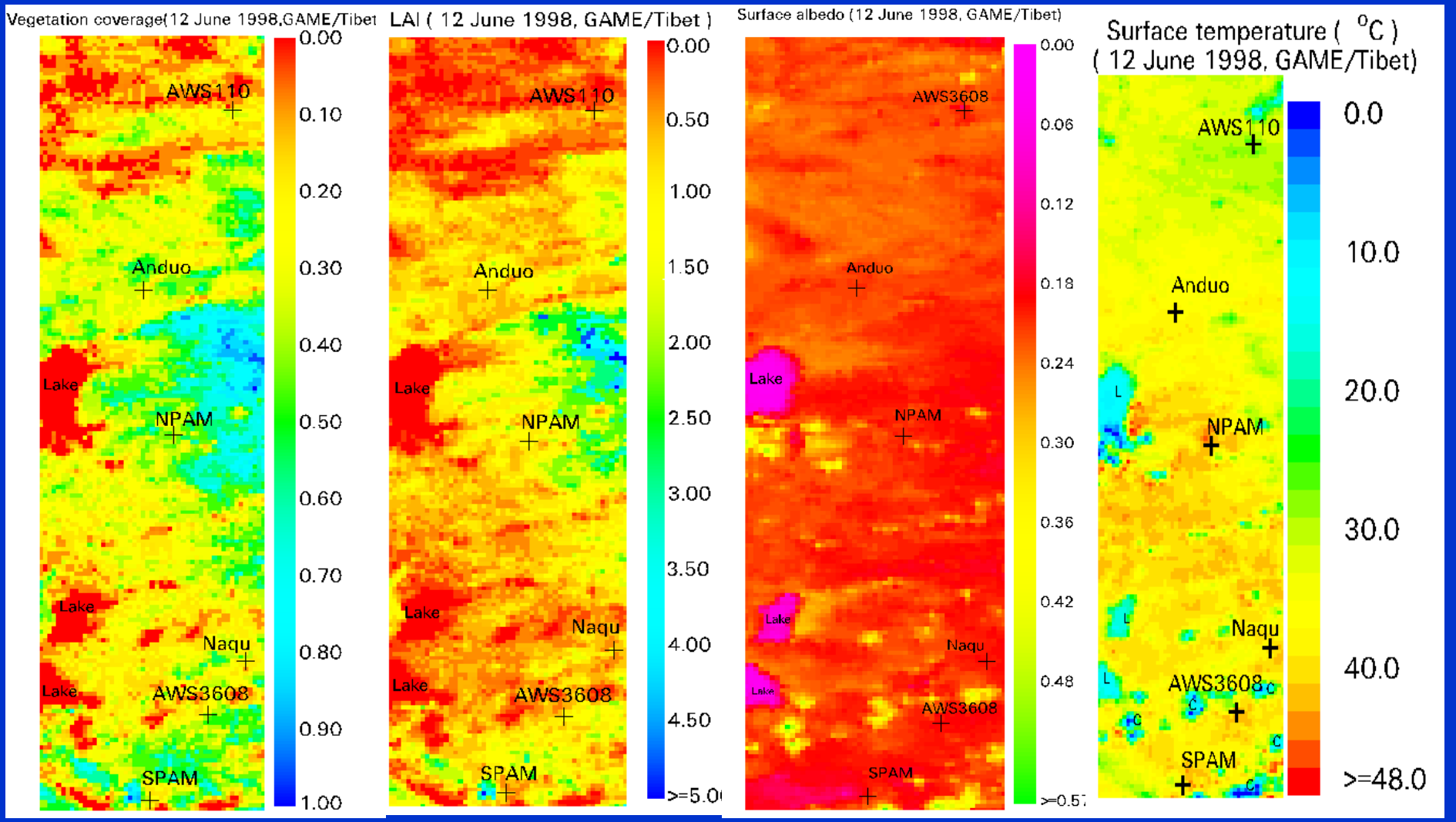

Net radiation

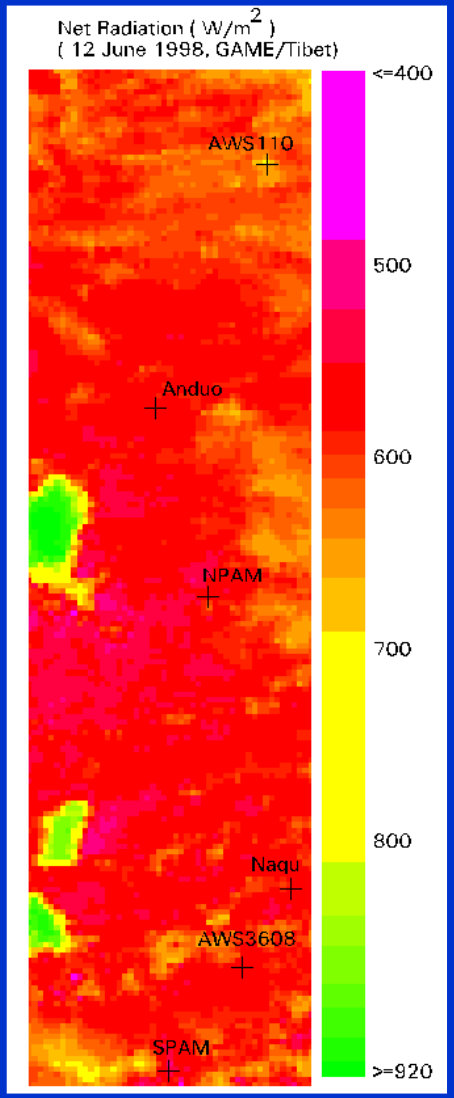

Soil heat flux

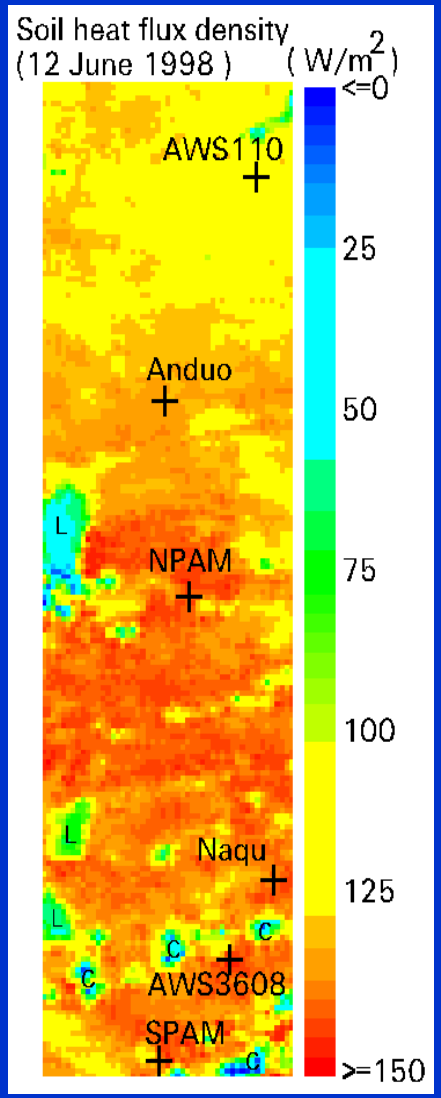

Sensible heat flux

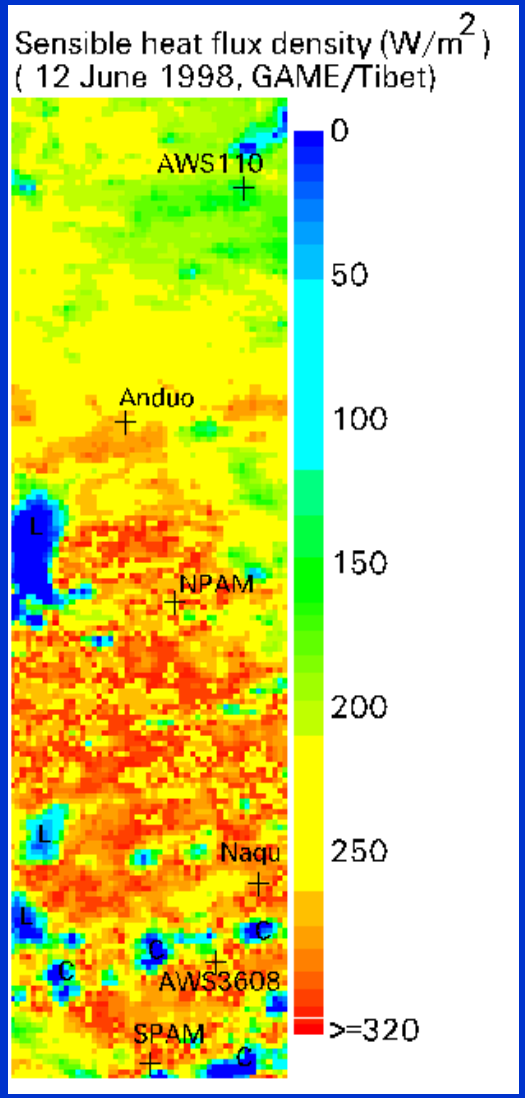

Latent heat flux

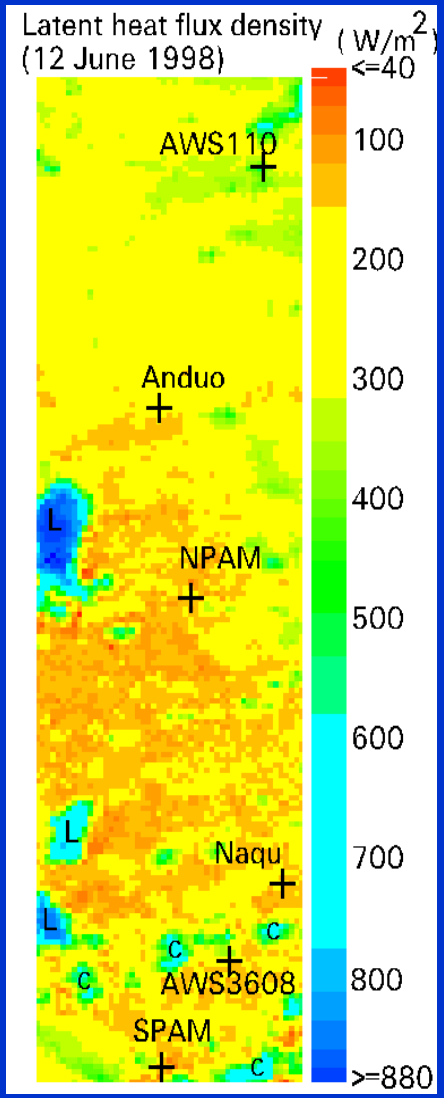

	June 12 (pre-Monsoon)	July 16 (Monsoon)	August 21 (Post-Monsoon)
NDVI	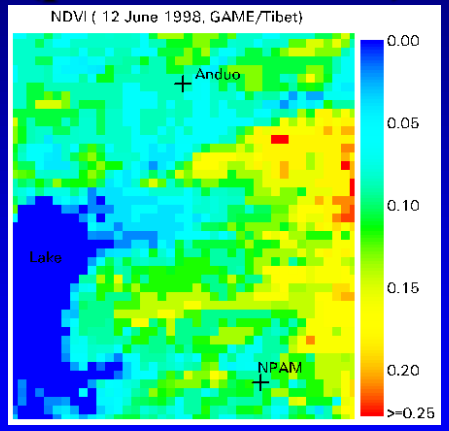	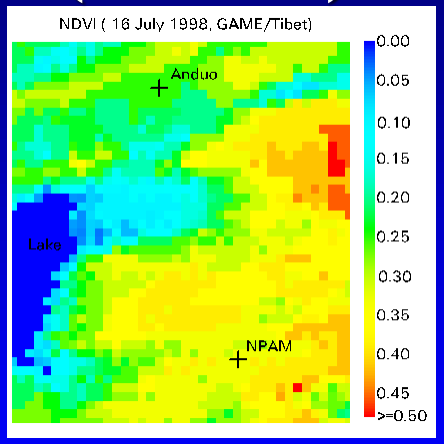	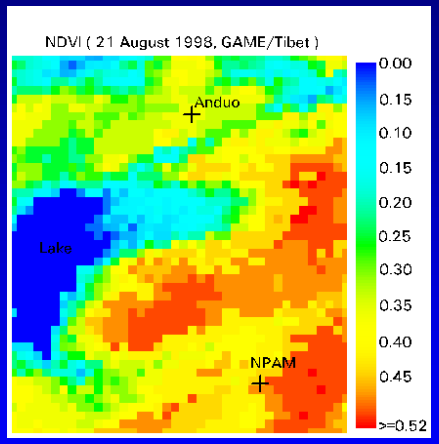
MSAVI	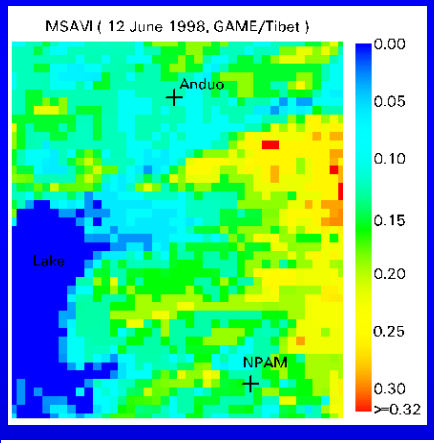	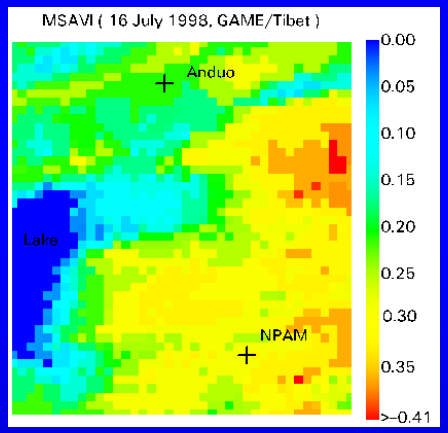	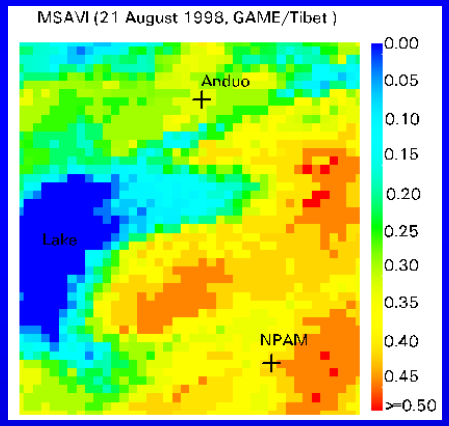
Vegetation coverage	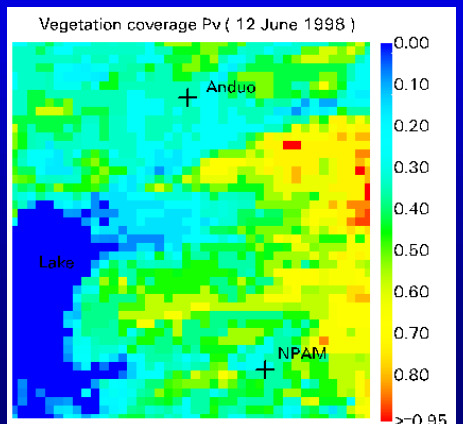	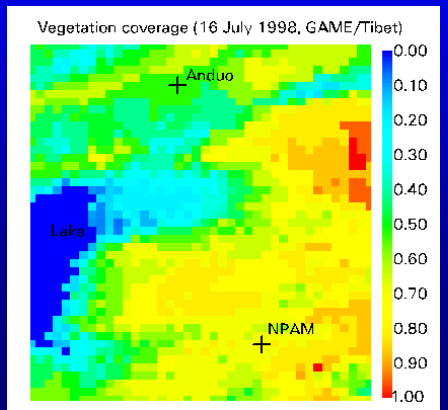	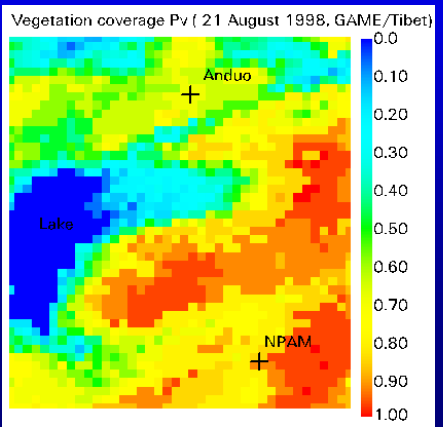

June

July

August

LAI

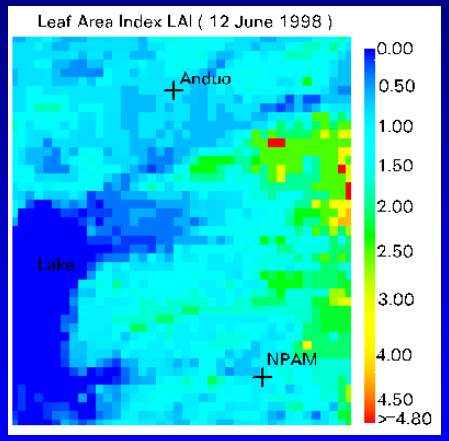

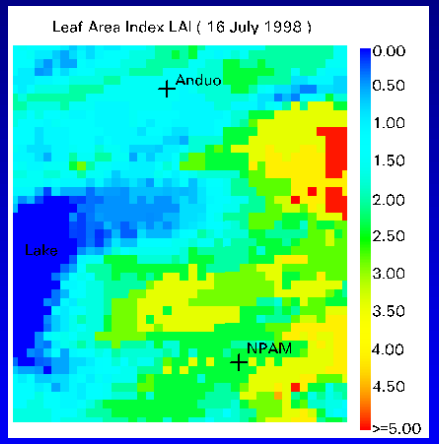

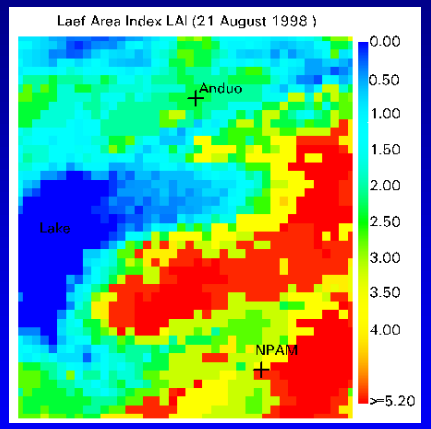

Surface reflectance

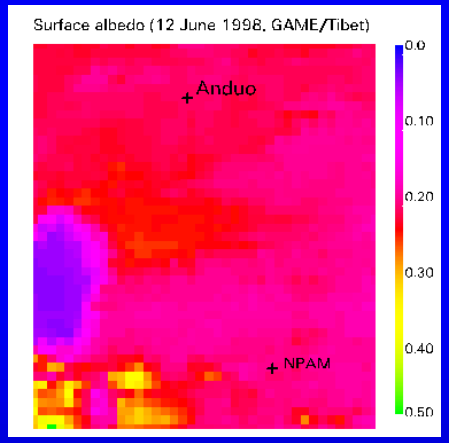

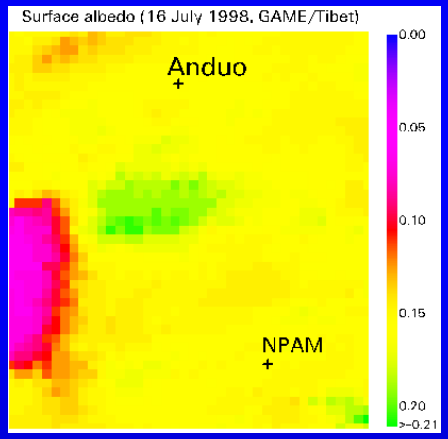

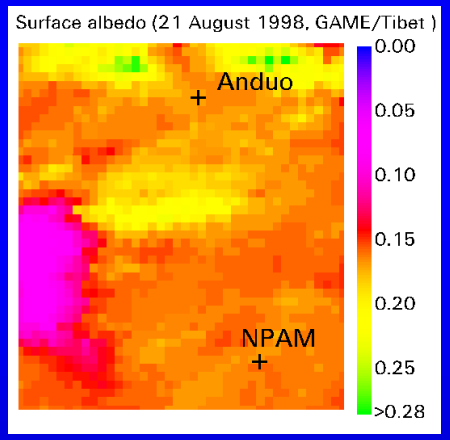

Surface temperature

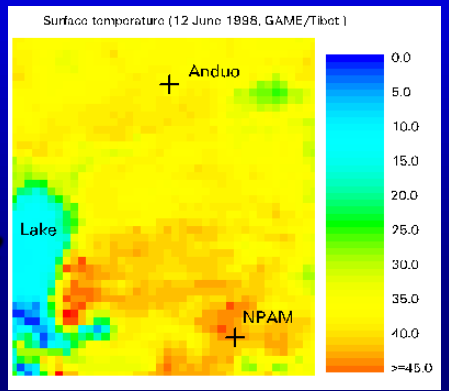

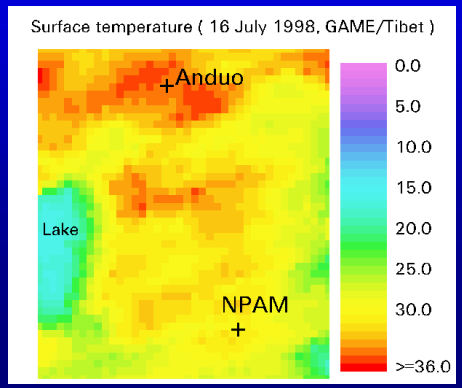

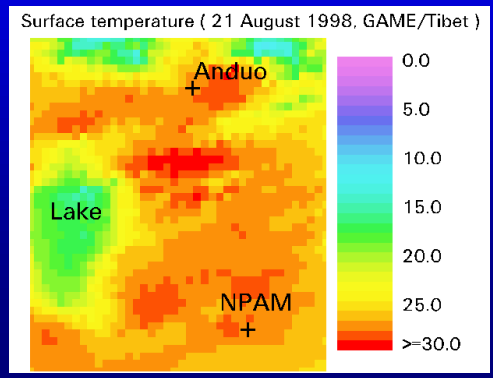

June

July

August

Net radiation

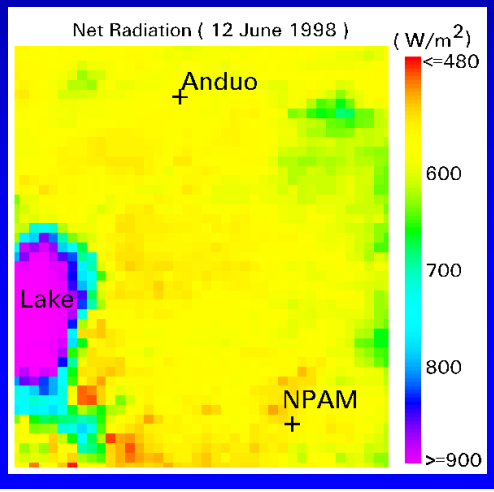

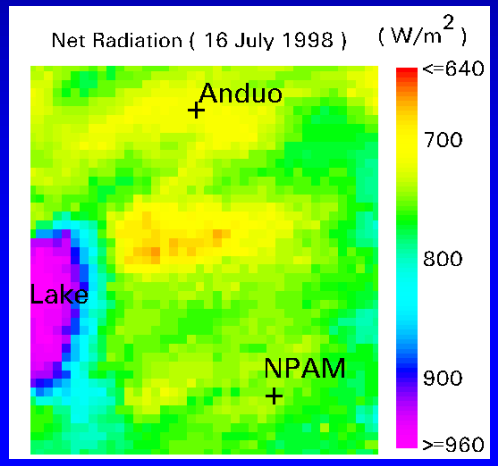

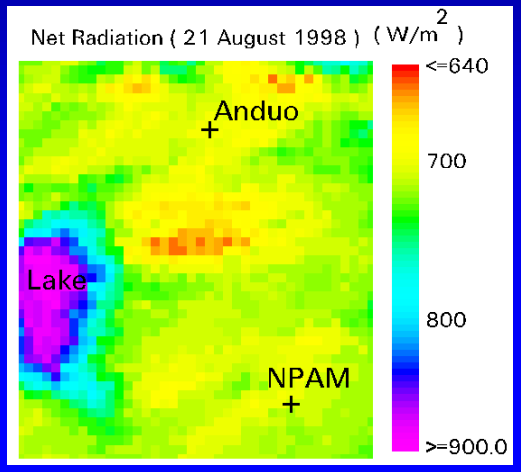

Soil heat flux

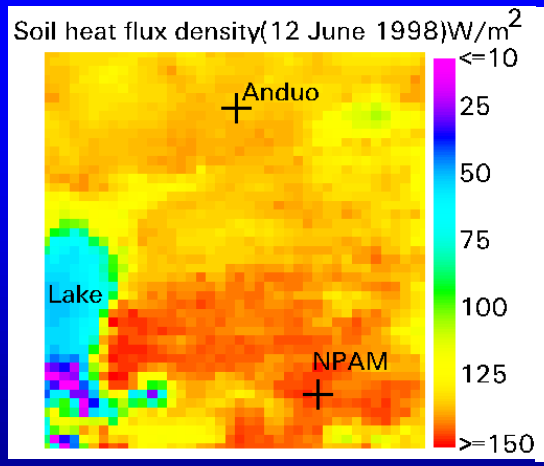

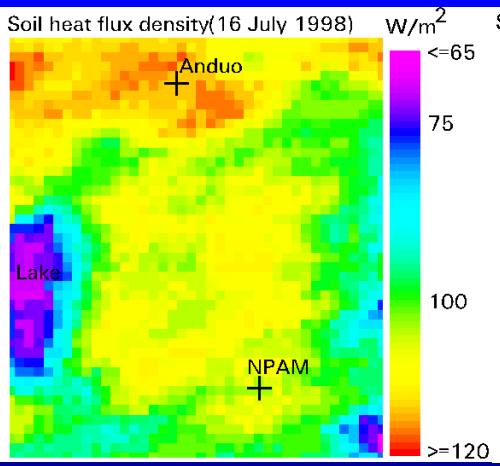

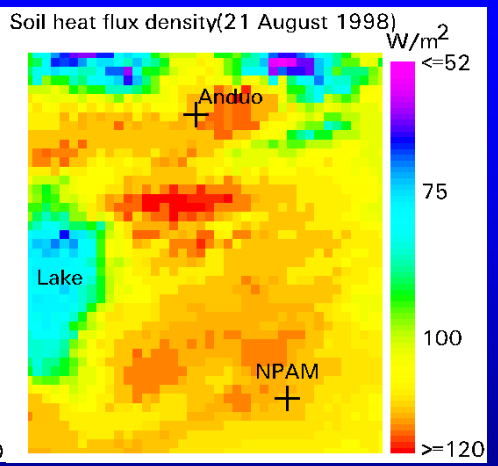

June July August

Sensible heat flux

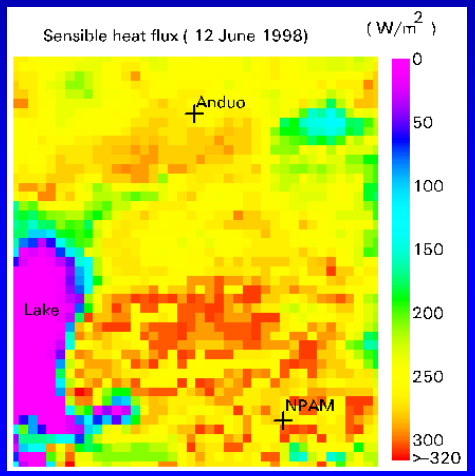

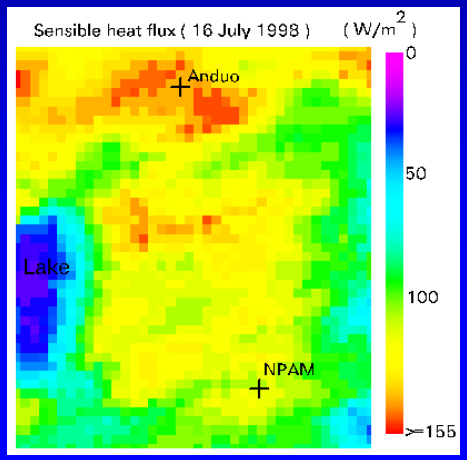

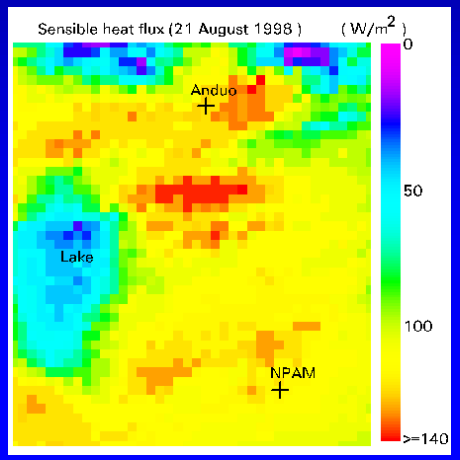

Latent heat flux

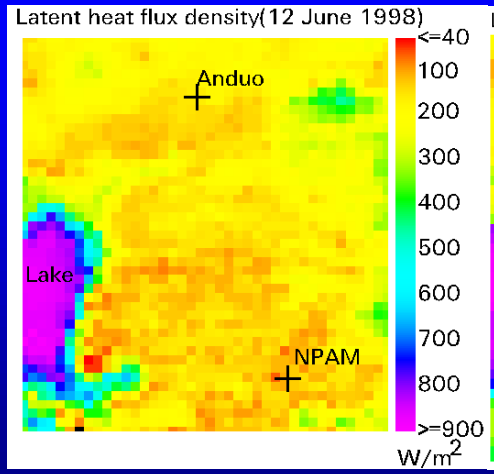

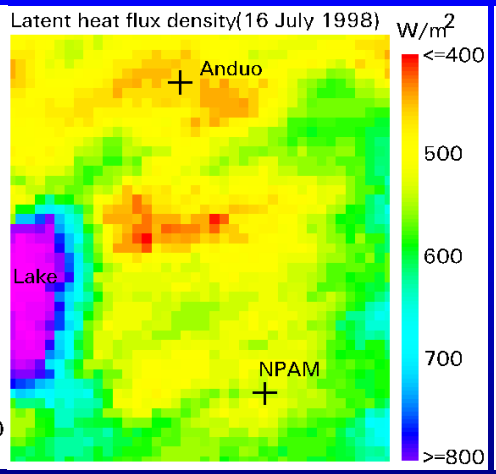

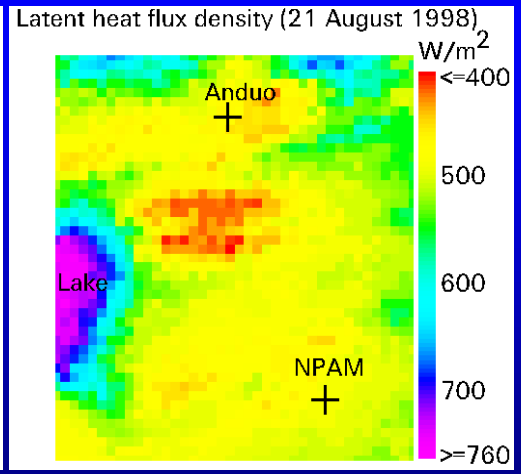

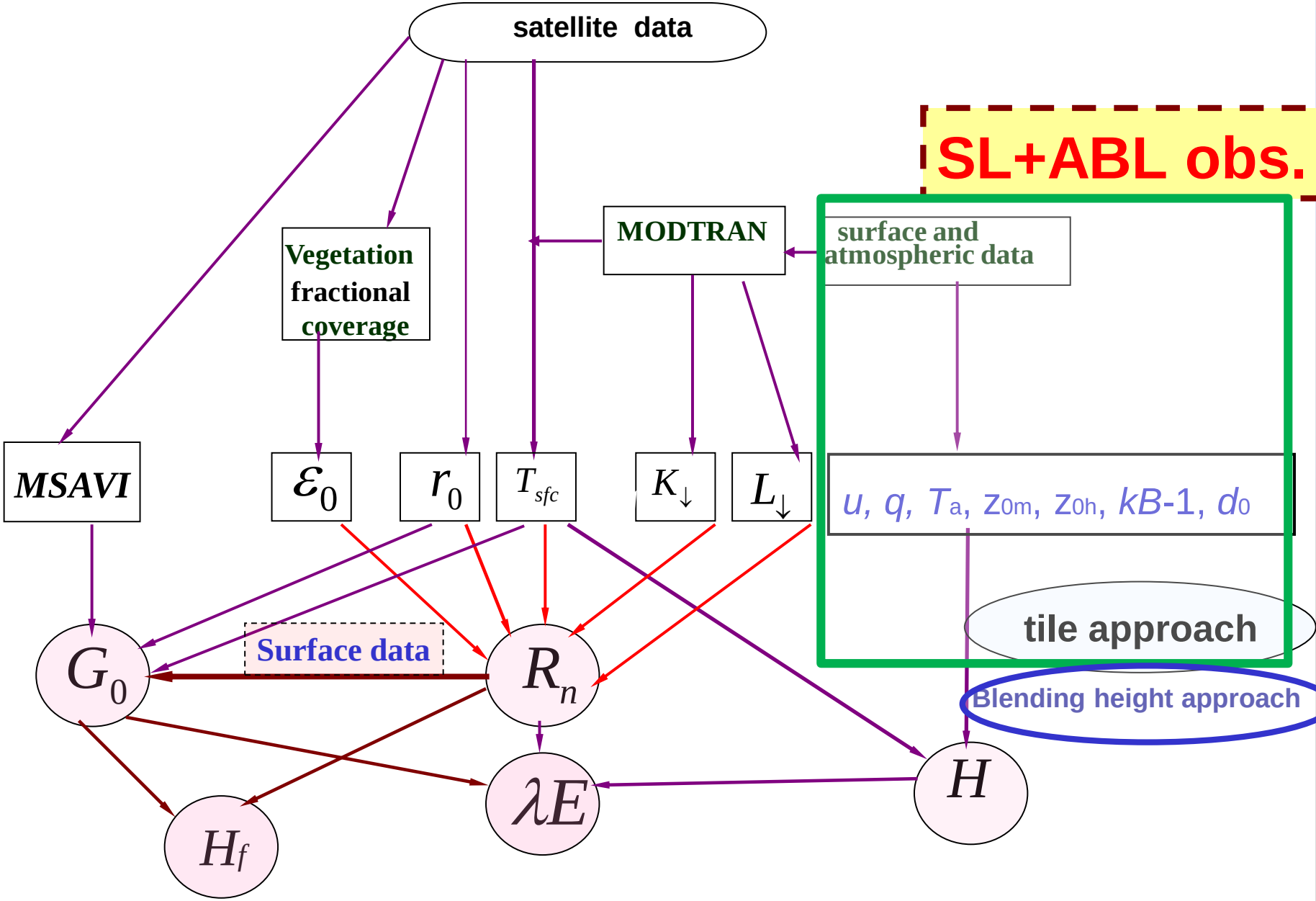

Fig.1 Diagram of parameterization procedure by MODIS data with field observations (Ma et al., 2011, AAS; Ma et al., 2014, ACP)

NDVI

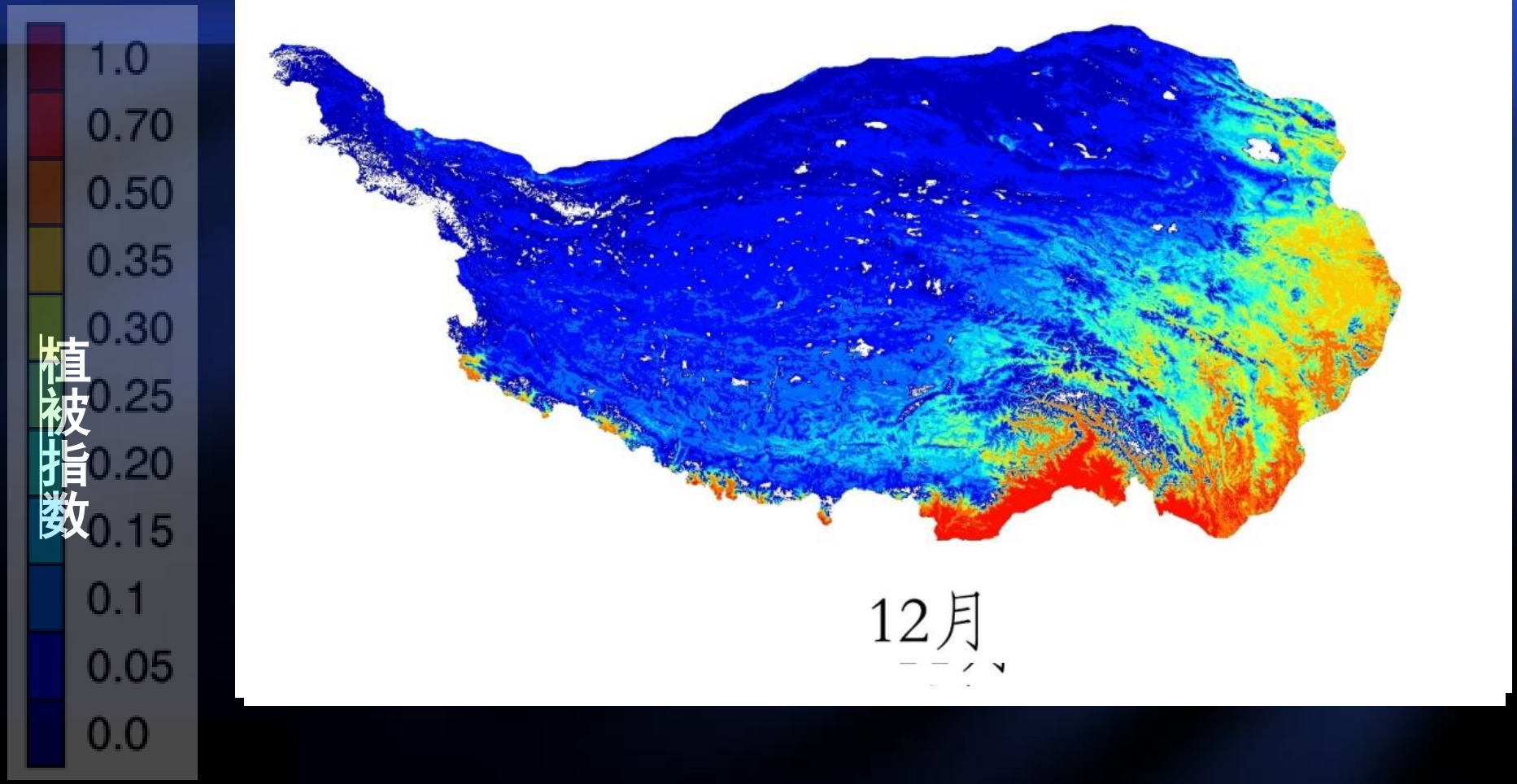

(Zhong et al. 2010,Climatic Change)

Surface temperature

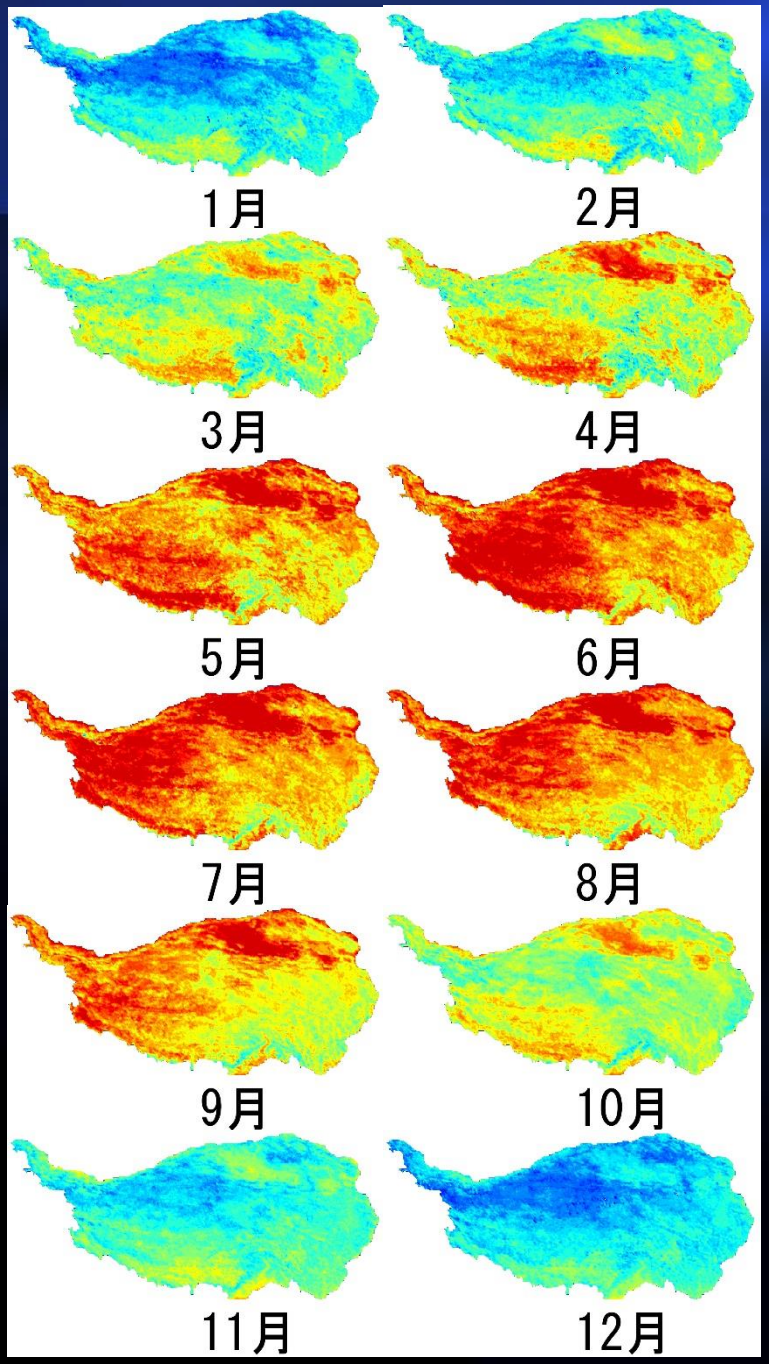

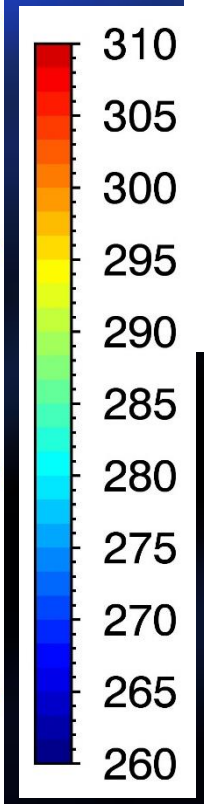

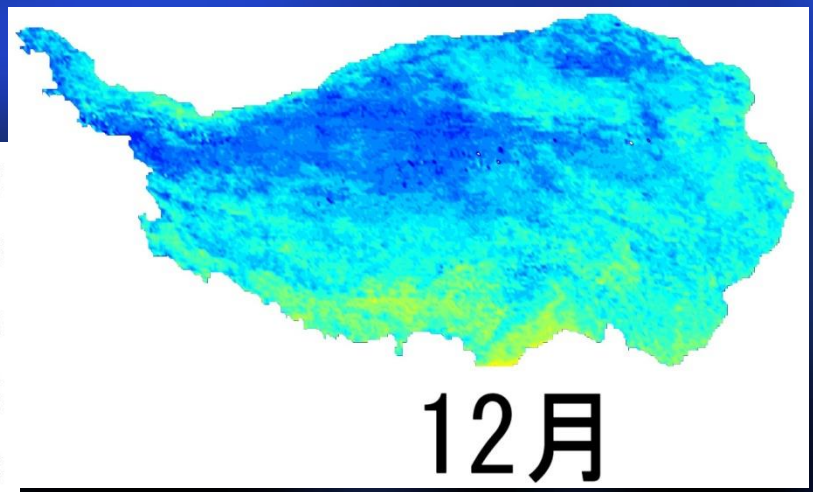

(Zhong and Ma et al. 2011,JC)

Latent heat flux

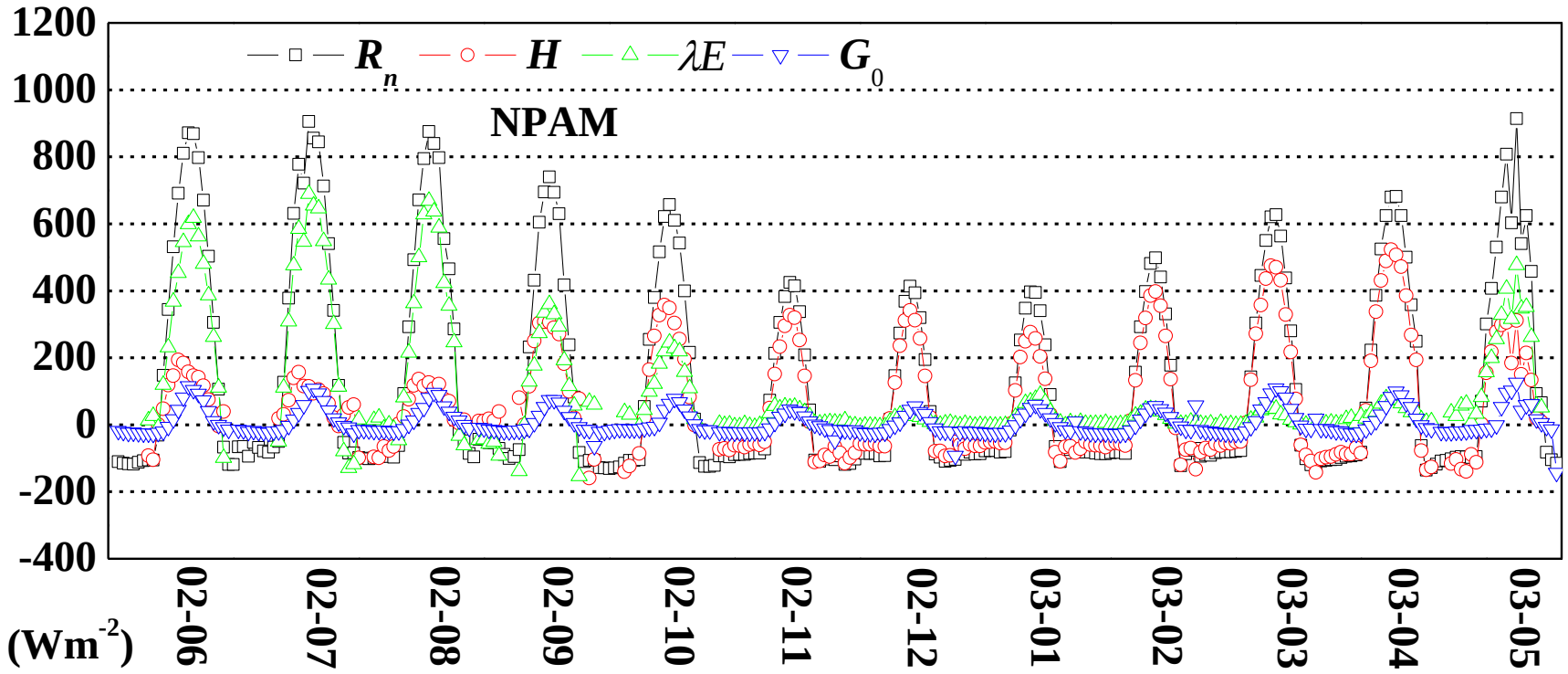

(Ma et al., 2014,ACP)

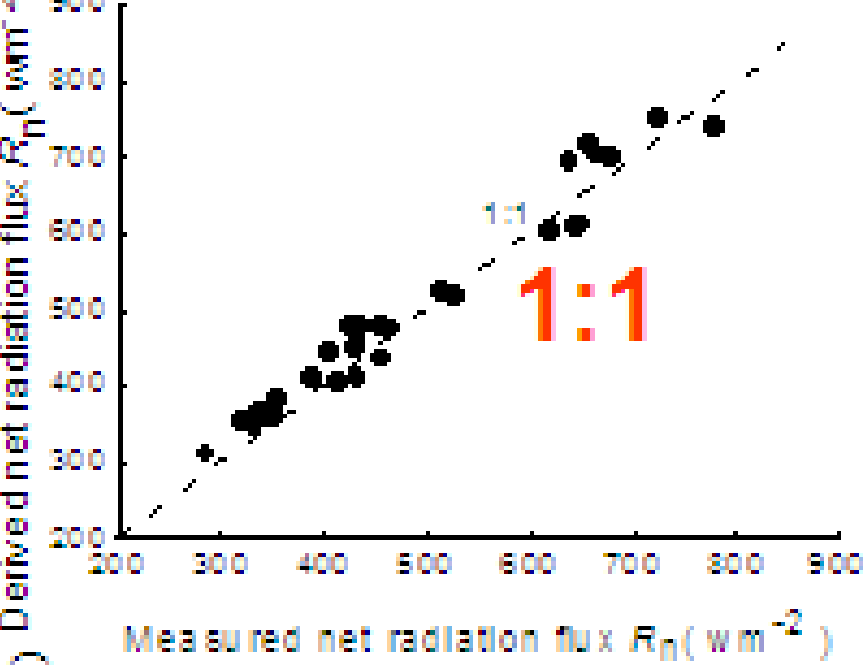
1:1
1:1
Derived net radiation flux R_n(wm^{-2})
Measured net radiation flux R_n(wm^{-2})

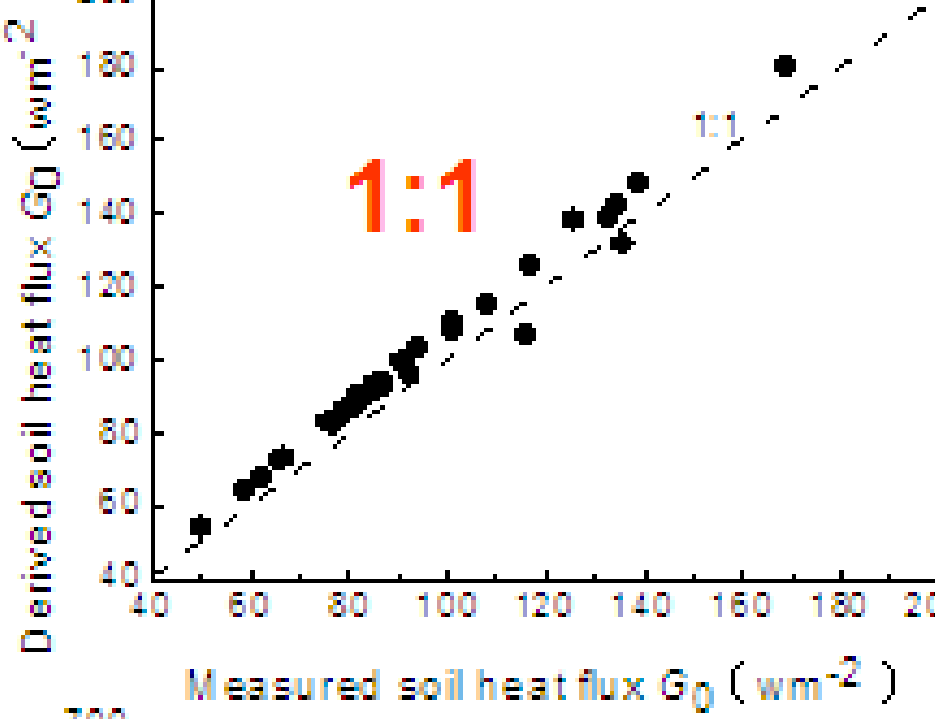
1:1
1:1
Derived soil heat flux G_0 (wm^{-2})
Measured soil heat flux G_0 (wm^{-2})

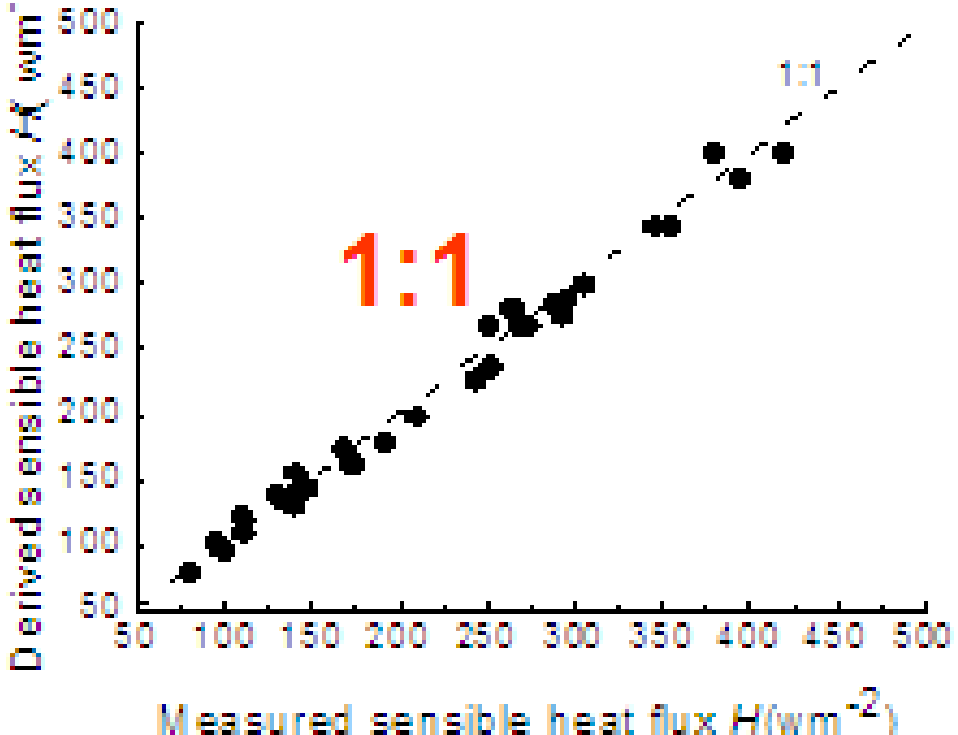
1:1
1:1
Derived sensible heat flux H(wm^{-2})
Measured sensible heat flux H(wm^{-2})

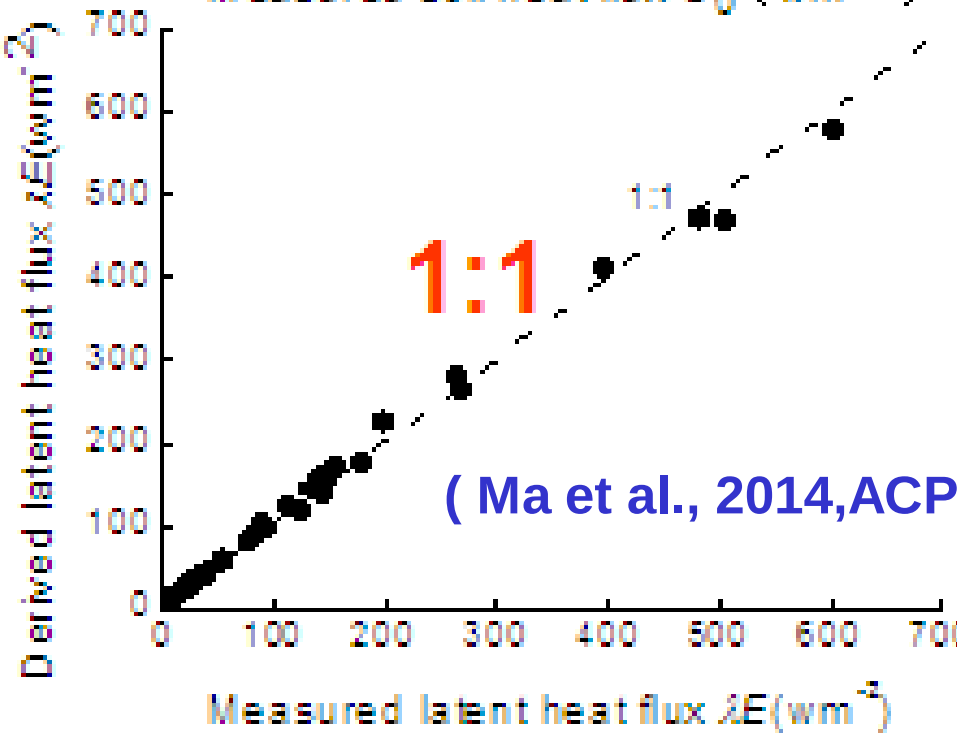
1:1
1:1
Derived latent heat flux λE(wm^{-2})
Measured latent heat flux λE(wm^{-2})
(Ma et al., 2014,ACP

(Han and Ma, 2015)

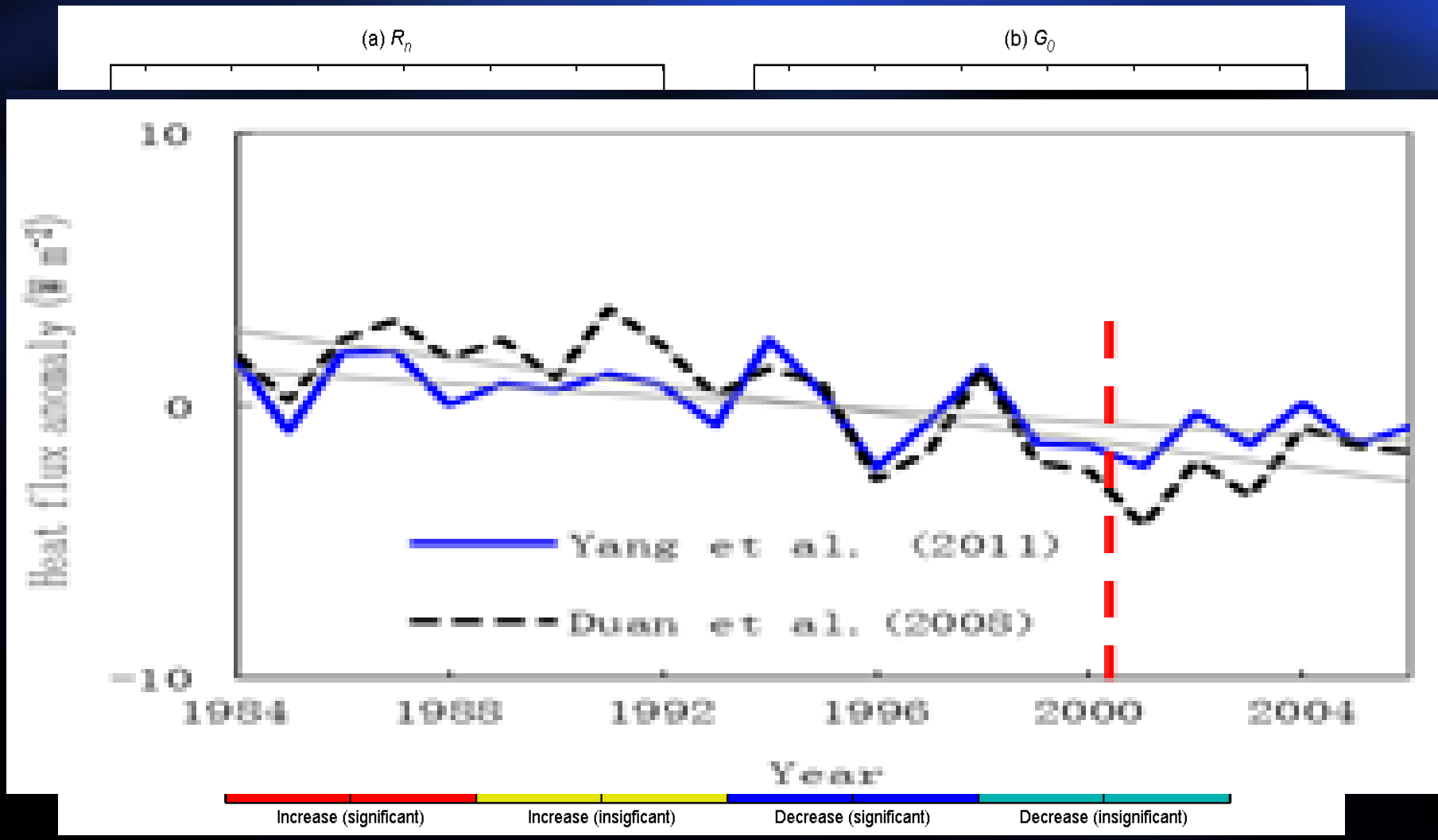

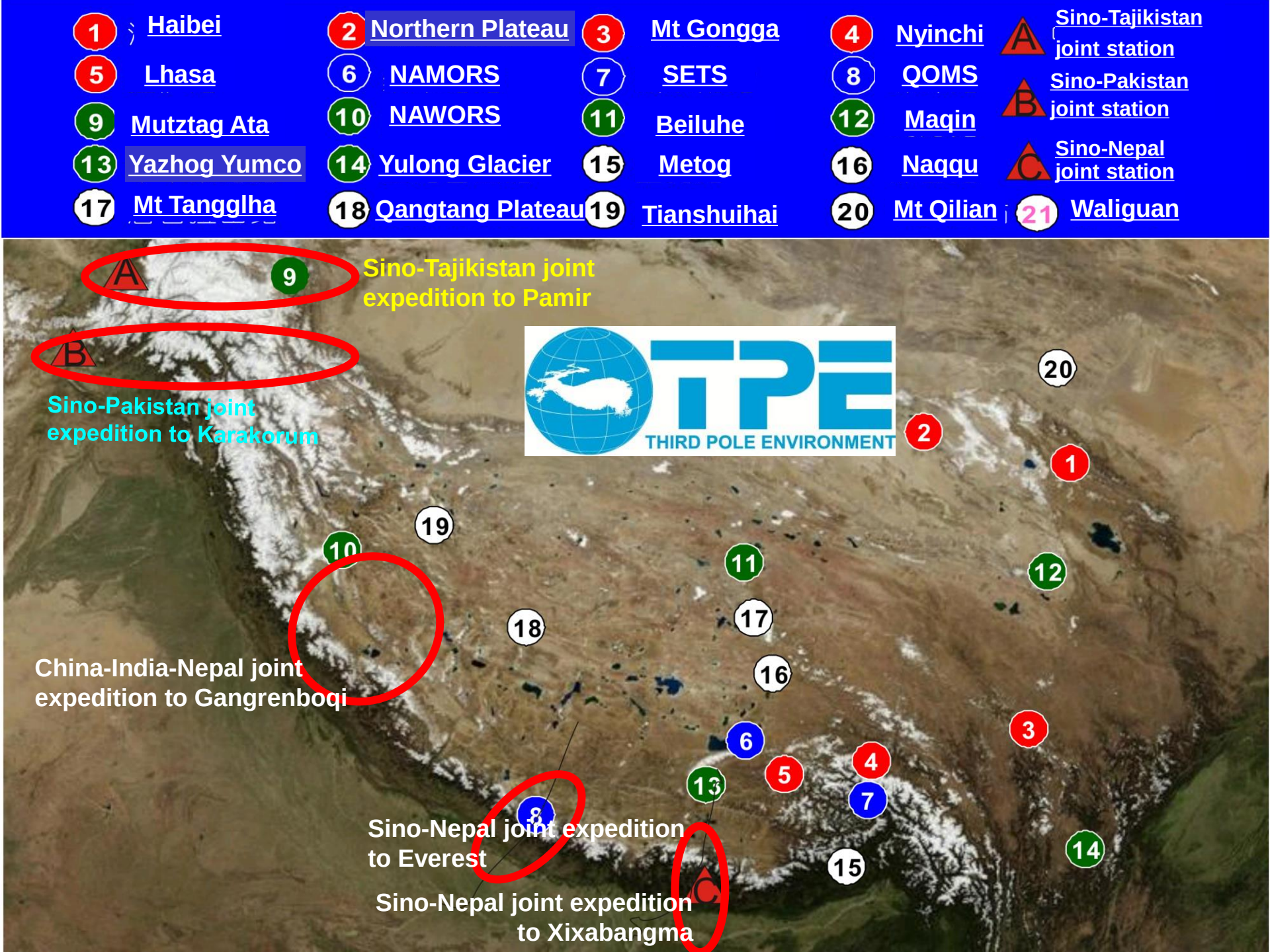
1 Haibei
2 Northern Plateau
3 Mt Gongga
4 Nyinchi
A Sino-Tajikistan joint station
5 Lhasa
6 NAMORS
7 SETS
8 QOMS
B Sino-Pakistan joint station
9 Mutztag Ata
10 NAWORS
11 Beiluhe
12 Maqin
13 Yazhog Yumco
14 Yulong Glacier
15 Metog
16 Naqqu
C Sino-Nepal joint station
17 Mt Tanggiha
18 Qangtang Plateau
19 Tianshuihai
20 Mt Qilian
21 Waliguan
A
9
Sino-Tajikistan joint expedition to Pamir
B
Sino-Pakistan joint expedition to Karakorum
TPE
THIRD POLE ENVIRONMENT
China-India-Nepal joint expedition to Gangrenboqi
Sino-Nepal joint expedition to Everest
Sino-Nepal joint expedition to Xixabangma
C

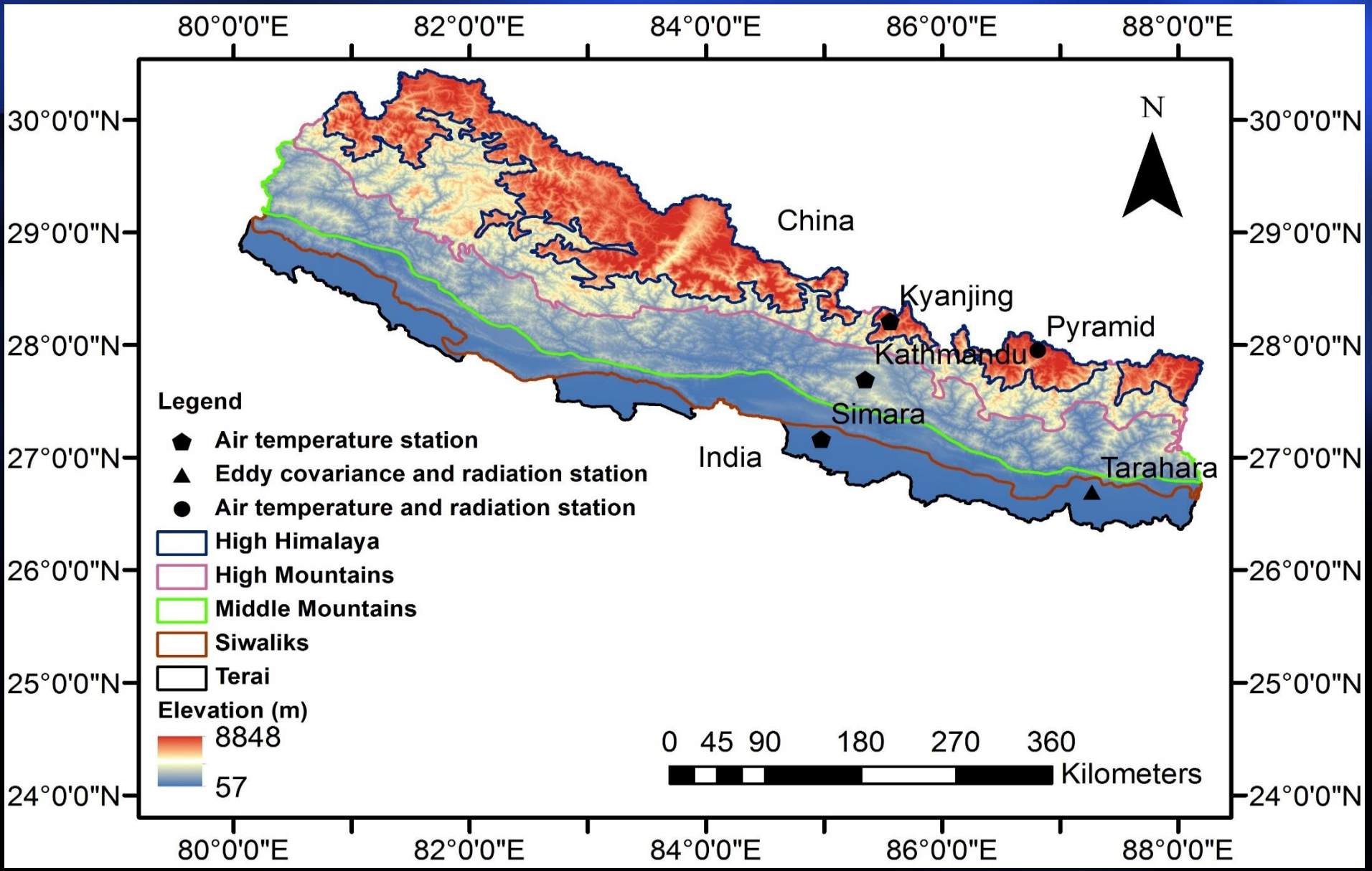
80°0'0"E
82°0'0"E
84°0'0"E
86°0'0"E
88°0'0"E
30°0'0"N
29°0'0"N
28°0'0"N
27°0'0"N
26°0'0"N
25°0'0"N
24°0'0"N
N
China
India
Kyanjing
Pyramid
Kathmandu
Simara
Tarahara
Legend
Air temperature station
Eddy covariance and radiation station
Air temperature and radiation station
High Himalaya
High Mountains
Middle Mountains
Siwaliks
Terai
Elevation (m)
8848
57
0 45 90 180 270 360
Kilometers

Heat fluxes distributions over Nepal

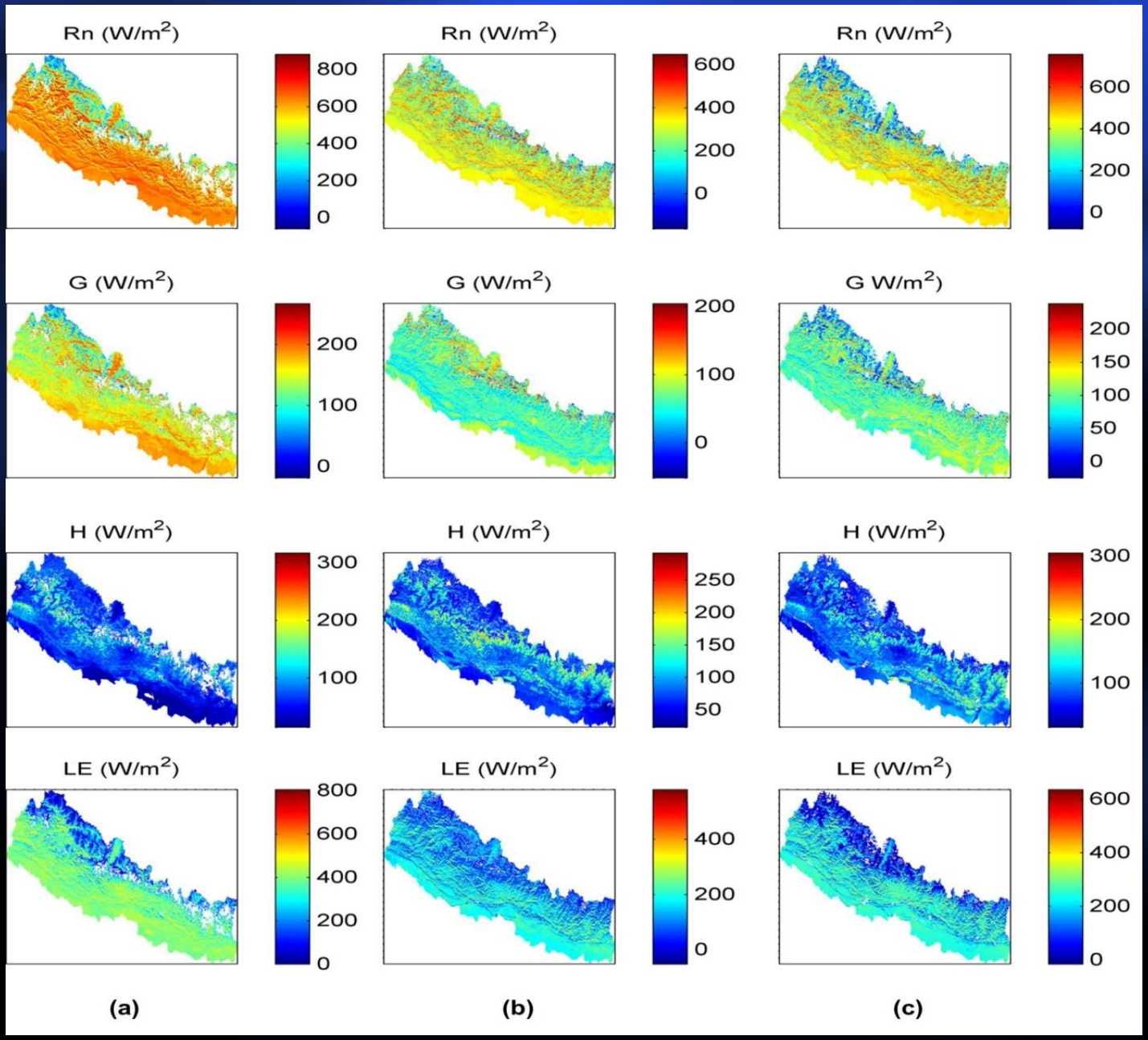

(Pukar and Ma et al.,2015,AR)

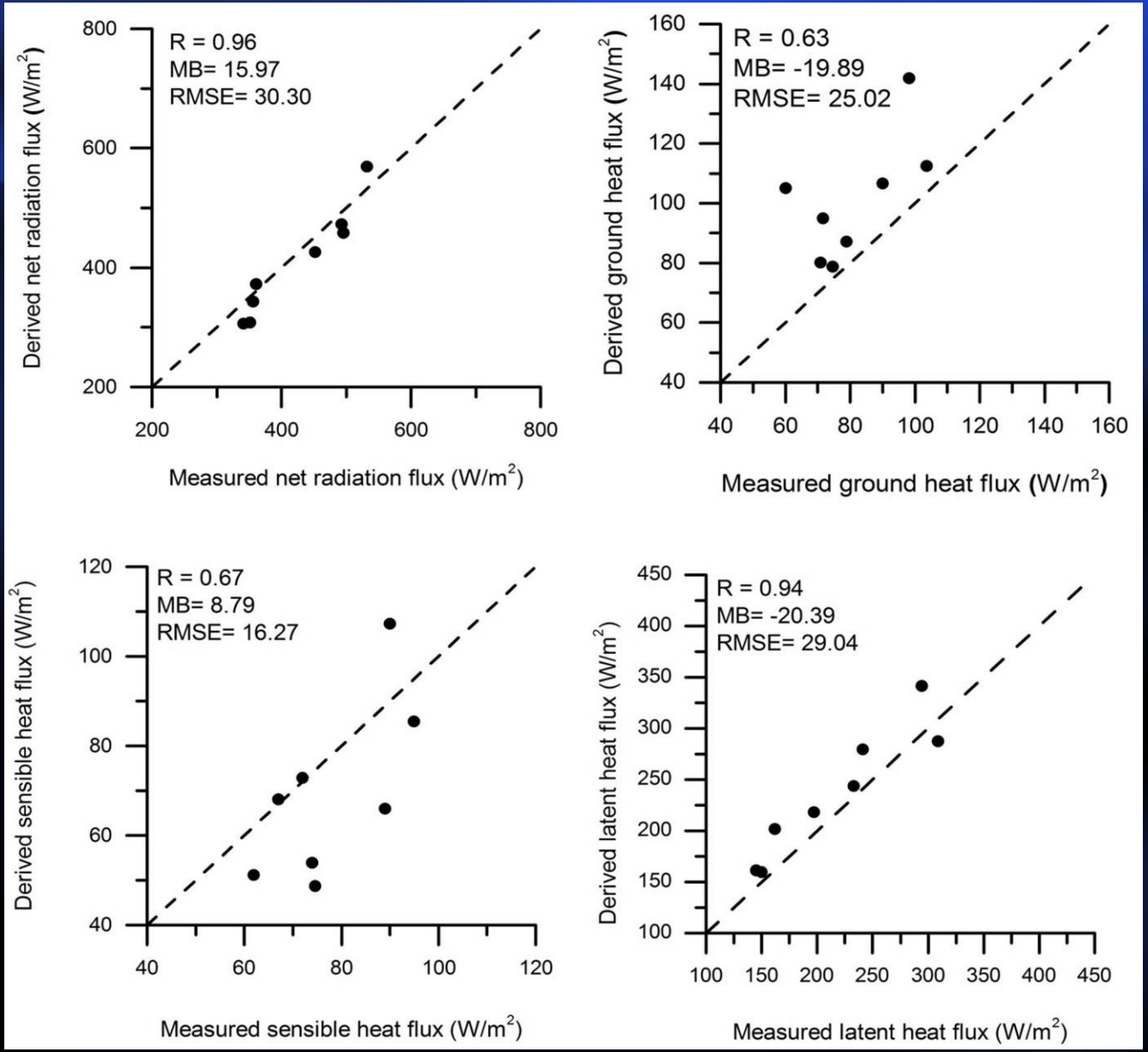

(Pukar and Ma et al.,2015,AR)

The variations of land surface heat fluxes for 11 years (2003–2013)

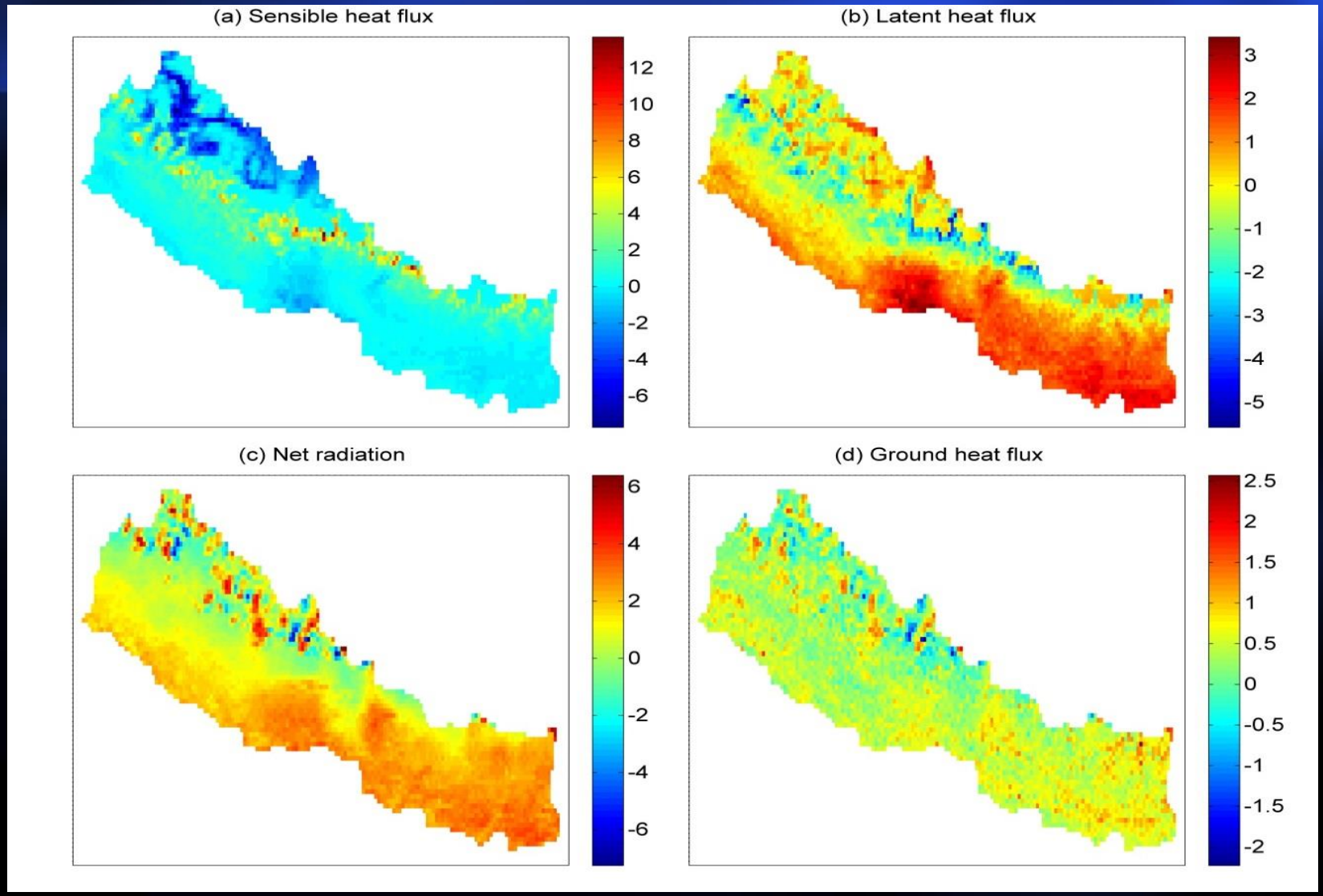

(Pukar and Ma et al., 2015, JGR)

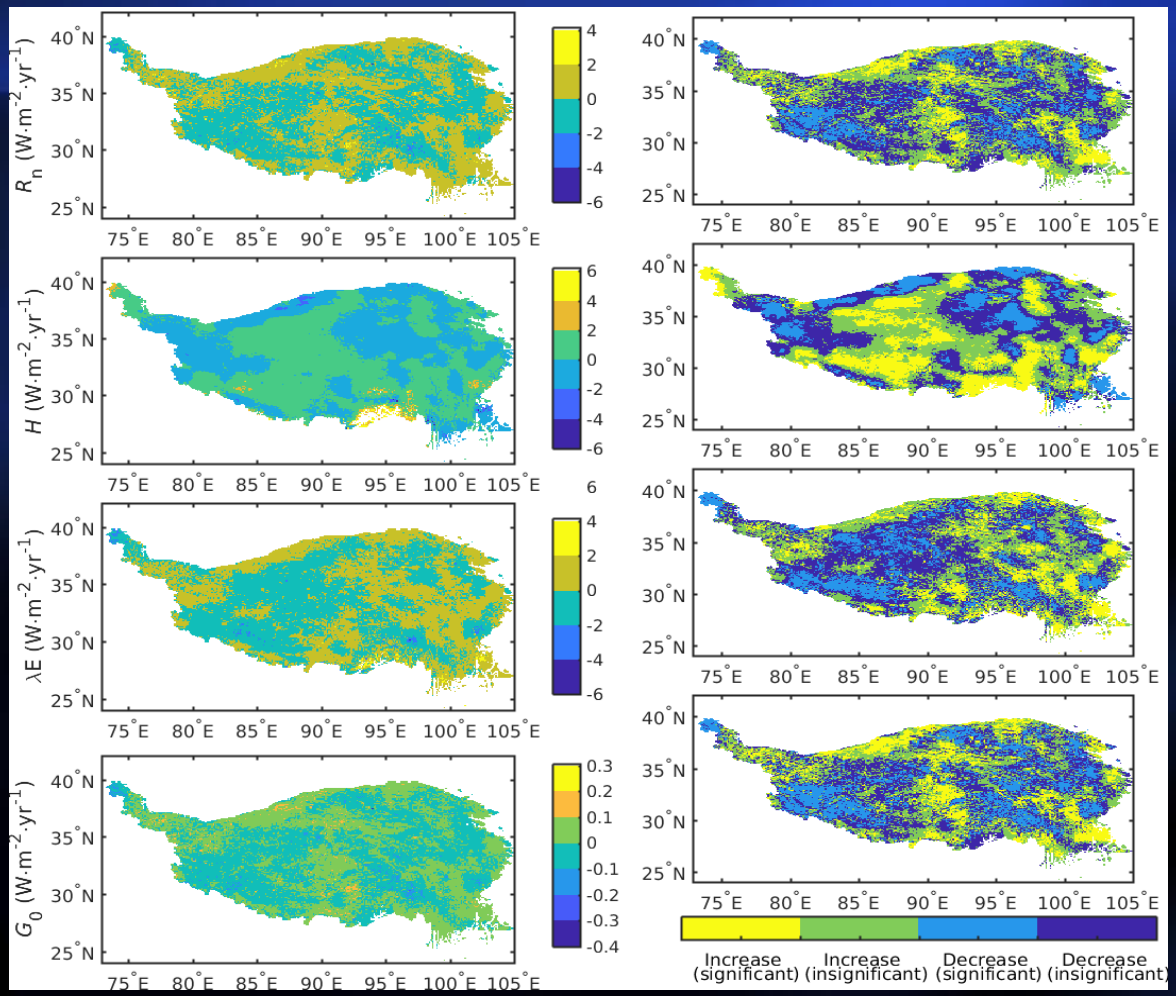

(2001-2016) (Ma et al, 2018,IJRS)

Thank you !

- Weiqiang Ma 马伟强
- Institute of Tibetan Plateau Research, Chinese Academy of Sciences
- 中国科学院青藏高原研究所
- Add: Building 3, Courtyard 16, Lincui Road. Chaoyang DistrictBeijing, 100101, China
- 北京朝阳区林萃路16号院3号楼
- Tel: +86-10-8409-7057 (O) / +86-180-1040-0029 (M)
- E-mail: wqma@itpcas.ac.cn